

First edition  
2009-05-15

---

---

**Determination of particle size  
distribution — Differential electrical  
mobility analysis for aerosol particles**

*Détermination de la distribution granulométrique — Analyse de mobilité  
électrique différentielle pour les particules d'aérosol*



Reference number  
ISO 15900:2009(E)

© ISO 2009

**PDF disclaimer**

This PDF file may contain embedded typefaces. In accordance with Adobe's licensing policy, this file may be printed or viewed but shall not be edited unless the typefaces which are embedded are licensed to and installed on the computer performing the editing. In downloading this file, parties accept therein the responsibility of not infringing Adobe's licensing policy. The ISO Central Secretariat accepts no liability in this area.

Adobe is a trademark of Adobe Systems Incorporated.

Details of the software products used to create this PDF file can be found in the General Info relative to the file; the PDF-creation parameters were optimized for printing. Every care has been taken to ensure that the file is suitable for use by ISO member bodies. In the unlikely event that a problem relating to it is found, please inform the Central Secretariat at the address given below.



**COPYRIGHT PROTECTED DOCUMENT**

© ISO 2009

All rights reserved. Unless otherwise specified, no part of this publication may be reproduced or utilized in any form or by any means, electronic or mechanical, including photocopying and microfilm, without permission in writing from either ISO at the address below or ISO's member body in the country of the requester.

ISO copyright office  
Case postale 56 • CH-1211 Geneva 20  
Tel. + 41 22 749 01 11  
Fax + 41 22 749 09 47  
E-mail [copyright@iso.org](mailto:copyright@iso.org)  
Web [www.iso.org](http://www.iso.org)

Published in Switzerland

# Contents

Page

Foreword.....	iv
Introduction .....	v
<b>1 Scope .....</b>	<b>1</b>
<b>2 Terms and definitions.....</b>	<b>1</b>
<b>3 Symbols .....</b>	<b>4</b>
<b>4 General principle.....</b>	<b>5</b>
<b>4.1 Particle size classification with the DEMC.....</b>	<b>5</b>
<b>4.2 Relationship between electrical mobility and particle size .....</b>	<b>6</b>
<b>4.3 Measurement and data inversion.....</b>	<b>7</b>
<b>4.4 Transfer function of the DEMC.....</b>	<b>8</b>
<b>4.5 The charge distribution function.....</b>	<b>8</b>
<b>5 System and apparatus.....</b>	<b>9</b>
<b>5.1 General configuration.....</b>	<b>9</b>
<b>5.2 Components .....</b>	<b>10</b>
<b>6 Measurement procedures .....</b>	<b>11</b>
<b>6.1 Setup and preparation of the instrument .....</b>	<b>11</b>
<b>6.2 Pre-measurement checks .....</b>	<b>14</b>
<b>6.3 Measurement.....</b>	<b>14</b>
<b>6.4 Maintenance .....</b>	<b>15</b>
<b>7 Periodic tests and calibrations.....</b>	<b>16</b>
<b>7.1 Overview .....</b>	<b>16</b>
<b>7.2 Leak test .....</b>	<b>16</b>
<b>7.3 Zero tests .....</b>	<b>17</b>
<b>7.4 Flow meter calibration.....</b>	<b>17</b>
<b>7.5 Voltage calibration.....</b>	<b>17</b>
<b>7.6 Particle charge conditioner integrity test.....</b>	<b>18</b>
<b>7.7 Calibration for size measurement .....</b>	<b>18</b>
<b>7.8 Size resolution test.....</b>	<b>19</b>
<b>7.9 Number concentration calibration .....</b>	<b>20</b>
<b>8 Reporting of results.....</b>	<b>20</b>
<b>Annex A (informative) Particle charge conditioners and charge distributions .....</b>	<b>21</b>
<b>Annex B (informative) Particle detectors .....</b>	<b>29</b>
<b>Annex C (informative) Slip correction factor .....</b>	<b>33</b>
<b>Annex D (informative) Data inversion .....</b>	<b>37</b>
<b>Annex E (informative) Cylindrical DEMC .....</b>	<b>43</b>
<b>Annex F (informative) Size calibration of a DMAS with step-wise voltage change using particle size standards .....</b>	<b>49</b>
<b>Annex G (informative) Uncertainty .....</b>	<b>52</b>
<b>Bibliography .....</b>	<b>55</b>

## Foreword

ISO (the International Organization for Standardization) is a worldwide federation of national standards bodies (ISO member bodies). The work of preparing International Standards is normally carried out through ISO technical committees. Each member body interested in a subject for which a technical committee has been established has the right to be represented on that committee. International organizations, governmental and non-governmental, in liaison with ISO, also take part in the work. ISO collaborates closely with the International Electrotechnical Commission (IEC) on all matters of electrotechnical standardization.

International Standards are drafted in accordance with the rules given in the ISO/IEC Directives, Part 2.

The main task of technical committees is to prepare International Standards. Draft International Standards adopted by the technical committees are circulated to the member bodies for voting. Publication as an International Standard requires approval by at least 75 % of the member bodies casting a vote.

Attention is drawn to the possibility that some of the elements of this document may be the subject of patent rights. ISO shall not be held responsible for identifying any or all such patent rights.

ISO 15900 was prepared by Technical Committee ISO/TC 24, *Particle characterization including sieving*, Subcommittee SC 4, *Particle characterization*.

## Introduction

Differential electrical mobility classification and analysis of airborne particles has been widely used to measure a variety of aerosol particles ranging from nanometre-size to micrometre-size in the gas phase. In addition, the electrical mobility classification of charged particles can be used to generate mono-disperse particles of known size for calibration of other instruments. One notable feature of these techniques is that they are based on simple physical principles. The techniques have become important in many fields of aerosol science and technology, e.g. aerosol instrumentation, production of materials from aerosols, contamination control in the semiconductor industry, atmospheric aerosol science, characterization of engineered nanoparticles, and so on. However, in order to use electrical mobility classification and analysis correctly, several issues, such as the slip correction factor, the ion-aerosol attachment coefficients, the size-dependent charge distribution on aerosol particles and the method used for inversion of the measured mobility distribution to the aerosol size distribution, need due caution.

There is, therefore, a need to establish an International Standard for the use of differential electrical mobility analysis for classifying aerosol particles. Its purpose is to provide a methodology for adequate quality control in particle size and number concentration measurement with this method.



# Determination of particle size distribution — Differential electrical mobility analysis for aerosol particles

## 1 Scope

This International Standard provides guidelines on the determination of aerosol particle size distribution by means of the analysis of electrical mobility of aerosol particles. This measurement is usually called “differential electrical mobility analysis for aerosol particles”. This analytical method is applicable to particle size measurements ranging from approximately 1 nm to 1 µm. This International Standard does not address the specific instrument design or the specific requirements of particle size distribution measurements for different applications, but includes the calculation method of uncertainty. In this International Standard, the complete system for carrying out differential electrical mobility analysis is referred to as DMAS (differential mobility analysing system), while the element within this system that classifies the particles according to their electrical mobility is referred to as DEMC (differential electrical mobility classifier).

**NOTE** For differential electrical mobility measurements relating to Road Vehicle applications, please refer to relevant national and international standards. ISO Technical Committee TC 22, *Road vehicles*, is responsible for developing International Standards relating to road vehicles, components and measurements.

## 2 Terms and definitions

For the purposes of this document, the following terms and definitions apply.

### 2.1

#### **aerosol**

system of solid or liquid particles suspended in gas

### 2.2

#### **attachment coefficient**

attachment probability of ions and aerosol particles

### 2.3

#### **bipolar charger**

device to attain the equilibrium steady state of charging by exposing aerosol particles to both positive and negative ions within the device

### 2.4

#### **charge neutralization**

process that leaves the aerosol particles with a distribution of charges that is in equilibrium and makes the net charge of the aerosol nearly zero, which is usually achieved by exposing aerosol particles to an electrically neutral cloud of positive and negative gas charges

### 2.5

#### **condensation particle counter**

#### **CPC**

instrument that measures the particle number concentration of an aerosol

**NOTE 1** The sizes of particles detected are usually smaller than several hundred nanometres and larger than a few nanometres.

NOTE 2 A CPC is one possible detector for use with a DEMC.

NOTE 3 In some cases, a condensation particle counter may be called a condensation nucleus counter (CNC).

**2.6  
critical mobility**

instrument parameter of a DEMC that defines the electrical mobility of aerosol particles that exit the DEMC in aerosol form, which may be defined by the geometry, aerosol and sheath air flow rates, and electrical field intensity

NOTE Particles larger or smaller than the critical mobility migrate to an electrode or exit with the excess flow and do not exit from the DEMC in aerosol form.

**2.7  
differential electrical mobility classifier  
DEMC**

classifier that is able to select aerosol particles according to their electrical mobility and pass them to its exit

NOTE A DEMC classifies aerosol particles by balancing the electrical force on each particle with its aerodynamic drag force in an electrical field. Classified particles are in a narrow range of electrical mobility determined by the operating conditions and physical dimensions of the DEMC, while they can have different sizes due to difference in the number of charges that they have.

**2.8  
differential mobility analysing system  
DMAS**

system to measure the size distribution of submicrometre aerosol particles consisting of a DEMC, flow meters, a particle detector, interconnecting plumbing, a computer and suitable software

**2.9  
electrical mobility**

mobility of a charged particle in an electrical field

NOTE Electrical mobility can be defined as the migration velocity dependent on the strength of the electrical field, the mechanical mobility and the number of charges per particle.

**2.10  
electrometer**

device that measures electrical current ranging from about 1 femtoampere (fA) to about 10 picoamperes (pA)

**2.11  
equilibrium charge distribution**

charging condition for aerosol particles that is stable after exposure to bipolar ions for a sufficiently long period of time

NOTE Bipolar ions are positive and negative ions which are produced by either a radioactive source or a corona discharge.

**2.12  
Faraday-cup aerosol electrometer  
FCAE**

electrometer designed for the measurement of electrical charges carried by aerosol particles

NOTE A Faraday-cup aerosol electrometer consists of an electrically conducting and electrically grounded cup as a guard to cover the sensing element that includes aerosol filtering media to capture charged aerosol particles, an electrical connection between the sensing element and an electrometer circuit, and a flow meter.

**2.13****Knudsen number** $Kn$  [ISO]

ratio of gas molecular mean free path to the radius of the particle, which is an indicator of free molecular flow versus continuum gas flow

**2.14****laminar flow**

gas flow with no temporally or spatially irregular activity or turbulent eddy flow

**2.15****migration velocity**

steady-state velocity of a charged airborne particle within an externally applied electric field

**2.16****particle charge conditioner**

device used to establish a known size-dependent charge distribution on the sampled aerosol of an unknown charging state, which is either a bipolar or unipolar charger

**2.17****Peclet number** $Pe$  [ISO]

dimensionless number representing the ratio of a particle's convective to diffusive transport

**2.18****Reynolds number** $Re$  [ISO]

dimensionless number expressed as the ratio of the inertial force to the viscous force; for example, applied to an aerosol particle or a tube carrying aerosol particles

**2.19****slip correction** $S_c$ 

dimensionless factor that is used to correct the drag force acting on a particle for non-continuum effects that become important when the particle size is comparable to or smaller than the mean free path of the gas molecules

**2.20****space charge**

net charge spatially distributed in a gas

**2.21****Stokes' drag**

drag force acting on a particle that is moving relative to a continuum fluid in the creeping flow (low Reynolds number) limit

**2.22****system transfer function**

transfer function defined as the ratio of the particle concentration at the particle concentration measurement detector of a DMAS to the particle concentration at the inlet of the DMAS, which is normally expressed as a function of electrical mobility

**2.23****transfer function**

ratio of particle concentration at the outlet of a DEMC to the particle concentration at the inlet of the DEMC, which is normally expressed as a function of electrical mobility

2.24

**unipolar charger**

device to attain a steady-state charge distribution of aerosol particles by exposing them to either positive or negative ions within the device

**3 Symbols**

For the purposes of this document, the following symbols are applied.

Symbol	Quantity	SI Unit
<i>A, B, C</i>	elements of the slip correction factor defined in Equation (2)	dimensionless
$C_N$	number concentration of an aerosol	$m^{-3}$
<i>c</i>	thermal velocity of an ion or molecule	$m s^{-1}$
<i>D</i>	diffusion coefficient of a particle or an ion in air	$m^2 s^{-3}$
<i>d</i>	aerosol particle diameter	m
<i>E</i>	electric field strength in a DEMC	$V m^{-1}$
$\varepsilon$	relative error	
<i>e</i>	elementary charge = $1,602\ 177 \times 10^{-19}$ C	
$K_n$	Knudsen number	
<i>k</i>	Boltzmann constant = $1,381 \times 10^{-23}$ J K <sup>-1</sup>	
<i>L</i>	effective active length of a DEMC, approximated by the axial distance between the midpoint of the aerosol entrance and the midpoint of the exit slit of a cylindrical DEMC	m
<i>l</i>	mean free path of a molecule	m
<i>M</i>	mass of a molecule	amu
<i>m</i>	mass of an ion	amu
$N_A$	Avogadro constant $\approx 6,022\ 141\ 79(30) \times 10^{23}$ mol <sup>-1</sup>	
$N_I$	number density of ions	$m^{-3}$
<i>P</i>	atmospheric pressure	Pa
<i>p</i>	number of elementary charges on a particle	(dimensionless)
<i>Pe</i>	Peclet number	(dimensionless)
$q_1, q_2, q_3, q_4$	flow rates of air (or gas) and of aerosol entering and exiting a DEMC	$m^3 s^{-1}$
$q_a$	aerosol air flow rate	
$r_1$	outer radius of inner cylinder of a cylindrical DEMC	m
$r_2$	inner radius of outer cylinder of a cylindrical DEMC	m
$Re$	Reynolds number	(dimensionless)
<i>S</i>	Sutherland constant ( =110,4 K at 23 °C and standard atmospheric pressure)	
$S_c$	slip correction	(dimensionless)
<i>T</i>	absolute temperature	K

Symbol	Quantity	SI Unit
$t$	residence time of an ion	s
$U$	DC voltage used to establish an electrical field in a DEMC	V
$V$	volume	m <sup>3</sup>
$Z$	electrical mobility of a charged aerosol particle	m <sup>2</sup> V <sup>-1</sup> s <sup>-1</sup>
$Z_1, Z_2, Z_3, Z_4$	critical electrical mobilities that describe the transfer function of a DEMC	m <sup>2</sup> V <sup>-1</sup> s <sup>-1</sup>
$\beta$	attachment coefficient of ions onto aerosol particles	m <sup>3</sup> s <sup>-1</sup>
$\gamma$	recombination coefficient of ions	(dimensionless)
$\delta$	radius of a limiting sphere	m
$\eta$	coefficient of dynamic viscosity of a gas	kg m <sup>-1</sup> s <sup>-1</sup>
$\iota$	ion pair production rate	m <sup>-3</sup> s <sup>-3</sup>
$\lambda$	mean free path of an ion	m
$\rho$	mass density of a particle	kg m <sup>-3</sup>

## 4 General principle

### 4.1 Particle size classification with the DEMC

The measurement of particle size distributions with a DMAS is based on particle classification by electrical mobility in a DEMC. The DEMC may be designed in many different ways; for example, coaxial cylindrical DEMC, radial DEMC, parallel plate DEMC, etc. The coaxial cylindrical DEMC shown in Figure 1 is an example of a widely used design. It consists of two coaxial, cylindrical electrodes with two inlets. One inlet (marked  $q_1$  in Figure 1) is for filtered clean sheath air. The other inlet (marked  $q_2$ ) is for the aerosol sample air.

The aerosol sample air, some of whose particles are electrically charged, enters the DEMC as a thin annular cylinder around a core of filtered, particle-free sheath air. By applying a voltage, an electric field is created between the inner and outer electrodes. A charged particle in the presence of an electric field will migrate within the field and reach a terminal migration velocity when the fluid dynamic drag on the particle balances the driving force of the electric field. Charged particles of the correct polarity within the sample air begin to drift across the sheath air flow towards the inner electrode. At the same time, the clean sheath air flow carries the charged airborne particles downward. A small fraction of the charged particles enters the thin circumferential slit near the bottom of the centre electrode and is carried by the air flow to the detector (in the direction marked  $q_3$ ). By varying the voltage, particles of different electrical mobility are selected.

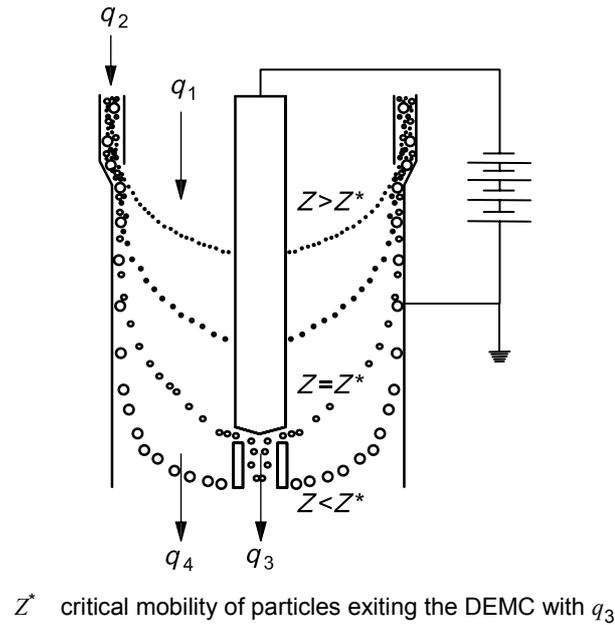


**Figure 1 — Schematic diagram of coaxial cylindrical DEMC**

When used within a DMAS, measurements of relevant parameters such as voltage and flow and their timings need to be combined with other measurements such as the output from the particle detector. These parameters are usually controlled using a system controller as shown in Figure 3.

**4.2 Relationship between electrical mobility and particle size**

The electrical mobility of a particle depends on its size and its electric charge. The relationship between electrical mobility and particle size for spherical particles can be described by Equation (1):

$$Z(d, p) = \frac{pe}{3\pi\eta d} S_c \tag{1}$$

The slip correction,  $S_c$ , extends the Stokes' law-based calculation of the drag force on a spherical particle moving with low Reynolds number in a gas phase to nanometre-sized particles. It is approximated by the expression given in Equation (2):

$$S_c = 1 + Kn \left[ A + B \exp\left(-\frac{C}{Kn}\right) \right] \tag{2}$$

For a detailed discussion of the slip correction, see Annex C.

The dynamic viscosity and the mean free path of gas molecules used within Equations (1) and (2), respectively, depend on both the temperature and the pressure of the carrier gas. Equations (3) and (4) shall be used to calculate the viscosity and the mean free path for temperatures and pressures different from the reference temperature and pressure,  $T_0$  and  $P_0$ , specified in Table 1, respectively.

$$\eta = \eta_0 \times \left(\frac{T}{T_0}\right)^{3/2} \times \left(\frac{T_0 + S}{T + S}\right) \tag{3}$$

$$l = l_0 \times \left(\frac{T}{T_0}\right)^2 \times \left(\frac{P_0}{P}\right) \times \left(\frac{T_0 + S}{T + S}\right) \tag{4}$$

where  $S$ , the Sutherland constant, has the value given in Table 1.

Unless explicitly specified differently in the measurement report, Equations (1) to (4) and the set of parameters given in Table 1 shall be used for the calculation of the relation between electrical mobility and particle size in air.

**Table 1 — Values of parameters recommended for the calculation of the electrical mobility from the particle size in air**

Parameter	Value	Remarks
$\eta_0$	$1,832\ 45\ 10^{-5}\ \text{kg}\cdot\text{m}^{-1}\cdot\text{s}^{-1}$	For dry air at $T_0 = 296,15\ \text{K}$ ; $P_0 = 101,3\ \text{kPa}$ . All values from: J.H. Kim, G.W. Mulholland, S.R. Kukuck and D.Y.H. Pui (2005).
$l_0$	$6,730 \times 10^{-8}\ \text{m}$	
$S$	$110,4\ \text{K}$	
$A$	$1,165$	
$B$	$0,483$	
$C$	$0,997$	

### 4.3 Measurement and data inversion

For a given supply voltage,  $U$ , the response,  $R(U)$ , of the particle detector to aerosol particles entering the DEMC is given by Equation (5), which is called the basic equation for the response of the electrical mobility measurement:

$$R(U) = q_2 \sum_{p=1}^{\infty} \int_{d=0}^{\infty} n(d) \cdot f_p(d) \cdot \Omega[Z(d, p), \Delta\Phi(U)] W(d, p) dd \quad (5)$$

where

$W(d, p)$  is the factor relating the detector response to the rate of particles;

For condensation particle counters (CPCs), the response is particle number concentration and  $W(d, p) = \eta_{\text{CPC}}(d) q_{\text{CPC}}^{-1}$ , where  $\eta_{\text{CPC}}(d)$  is the size-dependent detection efficiency of the CPC and  $q_{\text{CPC}}$  is the measuring flow rate of the CPC.

For Faraday-cup aerosol electrometers (FCAEs), the response is current and  $W(d, p) = p e \eta_{\text{FCAE}}(d)$ , where  $\eta_{\text{FCAE}}(d)$  is the size-dependent detection efficiency of the FCAE.

$n(d) dd$  is the number concentration of aerosol particles in the diameter interval  $dd$  around  $d$ ;

$f_p(d)$  is the charging probability function (see 4.5 and Annex A);

$\Omega[Z(d, p), \Delta\Phi(U)]$  is the transfer function of the DEMC (see 4.4 and Annex E);

$Z(d, p)$  is the electrical mobility (see 4.2);

$\Delta\Phi(U)$  is a function of the supply voltage and the geometry of the DEMC (see 4.4 and Annex E).

If the transfer function,  $\Omega$ , the charge distribution function,  $f_p(d)$ , and the maximum particle size (see 5.2.1) are known, the particle size distributions can be calculated based on the measurements with a DEMC. Details of some methods of data inversion are described in Annex D.

#### 4.4 Transfer function of the DEMC

The transfer function,  $\Omega$ , of a DEMC is defined as the probability that an aerosol particle which enters the DEMC at the aerosol inlet will leave via the detector outlet. It depends on the particle's electrical mobility,  $Z$ , on the four volumetric flow rates, on the geometry of the DEMC and on the electrical field. The influence of the geometry and the electrical field on the transfer function is expressed by the term  $\Delta\Phi$ , which is a function of the geometry and the supply voltage of the DEMC. For a given supply voltage,  $\Delta\Phi$  is constant.

If particle inertia, Brownian motion, space charge and its image forces are neglected, the transfer function of a DEMC can be described as a truncated isosceles triangle with the half-width,  $\Delta Z$ , centred around the electrical mobility,  $Z^*$ , as in Figure 2.

A detailed discussion of the transfer function for the example of a coaxial cylindrical DEMC can be found in Annex E.

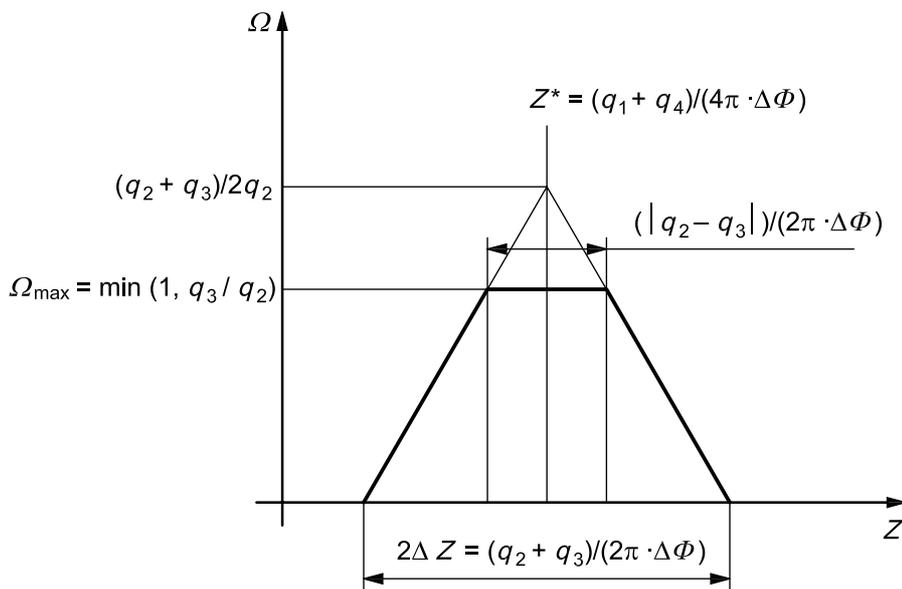


Figure 2 — Transfer function of a DEMC

#### 4.5 The charge distribution function

As stated in 4.3, the particle size-dependent charge distribution function,  $f_p(d)$ , must be known to calculate the particle size distribution of particles measured by a DEMC. In principle, a known charge distribution function can be established either by bipolar or by unipolar charging. An aerosol particle charge conditioner (5.2.2) is used for this purpose.

For unipolar charging, the achieved charge distribution depends on the technical design of the charger. Therefore, the charge distribution function,  $f_p(d)$ , must be evaluated for each specific unipolar charger design. The particle concentration to be charged must be limited in such a way that the depletion of the ion concentration due to ion attachment to the particles does not lead to significantly reduced charges on the particles. The instrument manufacturer or the user shall, by design or by measurement, ensure that the method performs correctly and does not produce artefact particles. Unipolar charging is discussed further in Annex A.

In a gaseous medium containing aerosol particles and a sufficiently high concentration of bipolar ions produced e.g. by a radioactive source, an equilibrium charge distribution will develop on the aerosol as a result of the random thermal motion of the ions and the frequent collisions between ions and aerosol particles. The bipolar equilibrium charge distribution depends on the ion properties (ion mobility and ion mass), gas-dynamic properties (diffusion coefficient of the ions and mean free path of the ions) and the ion-aerosol attachment coefficient. Details are described in Annex A.

The bipolar charging probability for spherical particles in air (293,15 K, 101,3 kPa) can also be calculated using the approximation by Wiedensohler (1988) <sup>[50]</sup> in combination with a result from Gunn (1956) <sup>[24]</sup>, given in Annex A. This approximation compares well both with other theoretical calculations and experimental results. Table 2 shows the results of this calculation.

Unless explicitly specified differently in the measurement report, values in Table 2 shall be used for the determination of the charge distribution function,  $f_p(d)$ , for aerosol particles in air.

**Table 2 — Bipolar charging probability  $f_p(d)$  for spherical particles in air (293,15 K, 101,3 kPa), from Equations (A.10) and (A.11)**

$d_p$ nm	Charging probability												
	-6	-5	-4	-3	-2	-1	0	1	2	3	4	5	6
1	0	0	0	0	0	0,004 8	0,999 3	0,004 5	0	0	0	0	0
2	0	0	0	0	0	0,008 3	0,974 2	0,007 5	0	0	0	0	0
5	0	0	0	0	0	0,022 5	0,969 3	0,018 9	0	0	0	0	0
10	0	0	0	0	0	0,051 4	0,912 4	0,041 1	0	0	0	0	0
20	0	0	0	0	0,000 2	0,109 6	0,793 1	0,084 6	0,000 1	0	0	0	0
50	0	0	0	0	0,011 4	0,222 9	0,581 4	0,169 6	0,006 6	0	0	0	0
100	0	0	0,000 1	0,003 7	0,056 1	0,279 3	0,425 9	0,213 8	0,031 7	0,001 7	0	0	0
200	0	0,000 5	0,005 3	0,034 0	0,121 1	0,264 1	0,299 1	0,204 3	0,071 9	0,015 3	0,001 8	0,000 1	0
500	0,006 7	0,020 7	0,050 4	0,098 0	0,149 0	0,181 6	0,181 8	0,140 3	0,089 1	0,044 0	0,017 3	0,005 4	0,001 4
1 000	0,035 7	0,058 4	0,085 4	0,111 3	0,126 1	0,138 5	0,123 5	0,103 9	0,075 4	0,050 0	0,029 3	0,015 4	0,007 2

## 5 System and apparatus

### 5.1 General configuration

A complete DMAS for the measurement of particle size distributions based on differential electrical mobility analysis typically has the following fundamental components (see Figure 3):

- pre-conditioner;
- particle charge conditioner;
- DEMC with flow control and high voltage control;
- aerosol particle detector;
- system controller with data acquisition and data analysis (typically built-in firmware or dedicated software on a personal computer).

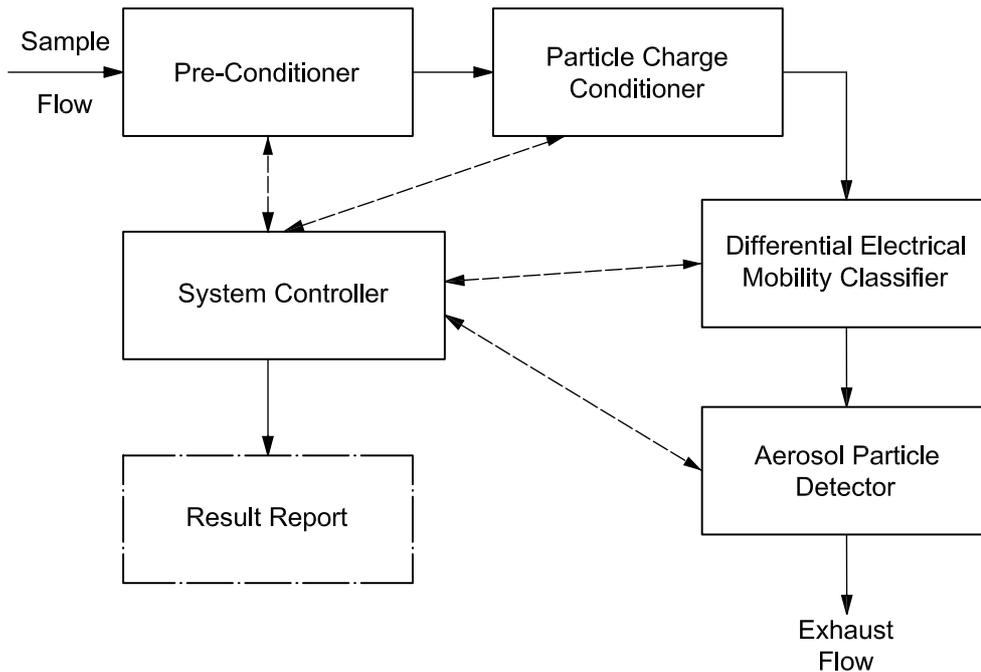


**Figure 3 — Fundamental components of the differential mobility analysing system (DMAS)**

Differential electrical mobility analysis is typically used for airborne particles ranging from a few nanometres to approximately one micrometre. Aerosol samples can be measured from a variety of sources. The most common sample sources are particles aerosolized from a liquid suspension, particles sampled directly from the atmosphere and particles sampled from a combustion source. The particle pre-conditioner and the particle charge conditioner are necessary to achieve defined sample conditions.

Most DMAS separate a mono-mobile fraction of the aerosol flow, which is transferred to the aerosol particle detector for particle number concentration measurement. In addition to the basic system configuration shown in Figure 3, other configurations exist, for example, systems with two parallel DEMCs and detectors for extended particle size range, systems with multiple detectors or systems with multiple parallel DEMCs and detectors.

The entire measurement is controlled by the system controller, which also acquires data and performs data inversion. The system control can, for example, reside as software and/or hardware in a personal computer. It can also be integrated into a self-contained particle sizing instrument.

## 5.2 Components

### 5.2.1 Pre-conditioner

The pre-conditioner component serves two purposes: removing large particles and, if necessary, reducing the sample humidity. Other pre-conditioning may be required for specific applications.

**NOTE** Calibrating the pressure differential across the particle pre-conditioner against the flow rate through this device is a helpful sampling flow measurement which does not interfere with the incoming particles.

### 5.2.2 Particle charge conditioner

In order to calculate the particle number distribution from the measured electrical mobility number distribution, the particle size-dependent distribution of electrical charges must be known. A bipolar diffusion particle charger (also called an aerosol neutralizer) is often used in a DMAS. The charger ionizes the aerosol carrier gas. The ions of both polarities diffuse to the aerosol particles, preferentially to particles of opposite polarity. Under appropriate operating conditions, these chargers establish the equilibrium charge distribution on the aerosol particles. Either radiation from a radioactive source or ions emitted from a corona electrode can be used to ionize the aerosol carrier gas. Unipolar corona chargers may also be used in a DMAS.

### 5.2.3 DEMC

The DEMC is the core component of a DMAS. The basic operating principle is electrical mobility discrimination by particle migration perpendicular to a laminar sheath flow. The migration is determined by an external electrical force and the counteracting particle drag forces in the laminar sheath flow.

DEMC can be designed in a variety of geometries. The classifying characteristic of a DEMC is described by its transfer function. Whatever the geometrical design of the DEMC, the transfer function is defined by the critical mobilities, which are determined by the geometrical dimensions of the device, by the flow rates and by the voltage potential between the electrodes. Details on the transfer function of the DEMC can be found in 4.4. For the example of a coaxial cylindrical DEMC, details on the critical mobilities as well as the transfer function can be found in Annex E.

Measuring a particle size distribution is usually achieved by changing the voltage. For transient measurements, DMASs with multiple particle detectors have been designed. These systems typically operate with fixed voltages.

### 5.2.4 Aerosol particle detector

The aerosol outlet from the DEMC shall be connected to a well-characterized particle detector. This instrument shall be able to detect particles exiting the DEMC with known efficiency across the entire size range to be reported. The lower end of the size range limits the aerosol particle detector that can be used.

Up to now, either a continuous flow condensation particle counter (CPC) or an aerosol electrometer have been used. In a CPC, aerosol particles are exposed to condensable supersaturated vapour. Vapour condensing on the particles grows them into droplets that can be counted by optical means. Aerosol electrometers are typically designed as Faraday-cup aerosol electrometers (FCAEs). The aerosol particles deposit on a filter inside the Faraday cup. The electrical charge on the deposited particles can be measured as a current by the electrometer amplifier. If there is no need to measure particles smaller than 100 nm, certain models of optical particle counters are also suitable as aerosol particle detectors.

Particle detectors are discussed further in Annex B.

### 5.2.5 System controller, data acquisition and analysis

The system controller with data acquisition and data inversion must cover several tasks. Before the measurement, the system control of an automated measuring system should set all operating parameters and flag the operator if any of these parameters cannot be set correctly. During the measurement, the system control should acquire and monitor all critical parameters (for example, the flow rates) and flag a warning to the operator if any of these parameters are outside pre-established tolerances. At the same time, the control system must set the electrode voltage through the variable high voltage supply and read the particle number data from the aerosol particle detector. Either during or after the measurement, data inversion takes place and the measured particle size distribution is presented, stored, exported, etc.

The system control should also create an event log which contains all detected irregularities during a measurement.

## 6 Measurement procedures

### 6.1 Setup and preparation of the instrument

#### 6.1.1 General

Proper instrument setup is critical in obtaining the correct particle size distribution. There are many different ways to configure and operate a DEMC instrument and the reader shall refer to the manufacturer's instrument manuals for specific details. This clause addresses only those issues common to all types of DEMC systems.

### 6.1.2 Aerosol pre-conditioning: Humidity

For atmospheric sampling, humidity may or may not play a role in obtaining an accurate particle size distribution. However, it shall be considered when making a measurement. Hygroscopic particles (e.g. sulfate particles) can change size depending on the amount of water in the air. Other types of particles (e.g. elemental carbon) will not be appreciably affected by humidity. Since humidity can change over time, the size distribution of the sample aerosol can also change over time. If sampling times are sufficiently long, the aerosol size distribution can change during a single measurement. This can be avoided by pre-drying the incoming aerosol with a diffusion dryer or by using dry dilution air. Other humidity control devices can allow measurements to be made at a constant relative humidity. In any case, it is important to consider how humidity may affect atmospheric aerosol measurements and how a dryer may affect particle losses.

Particles suspended in a liquid shall be thoroughly dried after atomization in order to obtain an accurate particle size distribution. The aerosol can be dried with dilution air (at less than 30 % relative humidity) or with a diffusion dryer. Dilution air is preferable if the aerosol concentration is very high and can tolerate dilution. If that is not the case, a diffusion dryer is the best choice.

### 6.1.3 Aerosol pre-conditioning: Separation of large particles

Measuring particle size distributions with a DMAS requires data inversion, as described in 4.3 and Annex D. In order to solve the inversion equations, it is necessary to know the size of the largest particles allowed to enter the DEMC. This will prevent larger multiply-charged particles from entering the DEMC. Large particles carrying multiple charges may have the same electrical mobility as smaller, singly-charged particles. By removing the larger particles, the true size distribution is more accurately determined.

A pre-separator with known cut-off sizes shall be installed in the sampling flow to fulfil this need. Commonly used pre-separators are impactors or cyclones. The cut-off size should be selected such that

- a) the pre-separator does not remove particles from the desired size range of the measurement, and
- b) the cut-off size is within the size range for data inversion.

NOTE Impactors are mostly used for sample flow rates of less than 1,5 l/min; cyclones are applicable for sample flow rates of 1 l/min and more.

During operation, some particles will deposit in the pre-separator. Therefore, the pre-separator needs to be regularly inspected and cleaned when necessary.

### 6.1.4 Particle charge conditioning

All aerosol samples should either be charge-neutralized or be charged unipolarly in a defined and reproducible way just before entering the DEMC.

Either radiation from a radioactive source <sup>1)</sup> or ions emitted from a corona electrode can be used to ionize the aerosol carrier gas. Three of the most common types of radioactive sources, <sup>241</sup>Am (primarily alpha radiation), <sup>85</sup>Kr (primarily beta radiation), and <sup>210</sup>Po (primarily alpha source) have half-lives of 458 years, 10,78 years and 138,4 days, respectively. It is especially important to ensure that the radioactive source is still strong enough to neutralize the incoming aerosol. A weak radioactive source or an improperly working charger will skew the particle size distribution, giving incorrect results. Under appropriate operating conditions, these chargers establish equilibrium charge distribution on the aerosol particles.

Unipolar charging can yield a higher charging probability than charge equilibrium, thus increasing the system transfer function. The increased charging probability, however, leads to both a higher fraction of multiply-charged particles and higher charge levels on these particles. This has the adverse effect of reducing the size resolution of the DEMC. Therefore, unipolar charging is typically used for instruments with lower size resolution.

---

1) Using radioactive sources requires compliance with local, national and international regulations and laws.

It is possible for any particle charge conditioner, particularly bipolar and unipolar corona chargers, to generate ultrafine particles that lead to incorrect measurement. Careful charger design, characterization and operation are necessary to minimize or avoid such effects.

Details of the charge equilibrium distribution can be found in 4.5. Details on particle charge conditioners can be found in Annex A.

#### 6.1.5 DEMC: Flows

The flow control system is an important component with respect to the precision, resolution and repeatability of a DEMC. Both the particle sizing and the particle concentration measurement rely on accurately known flows.

Depending on the type of DEMC used, the sheath flow to aerosol flow ratio will vary. A high sheath/aerosol ratio will result in a narrow transfer function with better resolution of the size distribution. A higher sheath flow rate also reduces diffusion broadening within the DEMC. A low sheath/aerosol ratio will increase the aerosol concentration, desirable for lower concentration aerosols.

Every DEMC has two flows entering the device (sample flow and sheath flow) and two flows exiting the device (monodisperse aerosol flow and excess air flow). Three out of these four flows must be controlled for stable operation. The sheath air shall be particle-free. In order to avoid interference with the aerosol to be measured, the recommended flows to be controlled are the sheath flow, the excess air flow and the monodisperse aerosol flow. Absolute accuracy on the flow rate measurements is critical since the sample flow is, in general, determined by the difference between the outgoing flows and the incoming sheath flow.

The inlet and outlet flows are strongly coupled, so upstream or downstream perturbations to any one of the flows may cause other flows to change. To minimize the sensitivity to such perturbations, the flow network should be carefully designed. The volumetric flow rates shall be defined and kept constant during the measurement. It should be periodically ensured that there are no leaks in the system.

The flow control system can be simplified and stabilized by cleaning and recirculation of the excess flow as sheath flow in a closed loop. This recirculation not only guarantees that the sheath flow equals the excess flow, it also eases the constraints on the precision with which the sheath and excess flow rates are measured since, in steady-state operation, the incoming aerosol flow exactly equals the outgoing classified monodisperse aerosol flow, provided there are no leaks in the recirculation system and the temperature of the recycled particle-free gas is the same as that of the incoming aerosol flow into the DEMC. An exception is a measuring setup where the aerosol inlet is pressurized (overpressure sampling mode). In such a case, it might become necessary to use a metered bleed to allow balancing of the flows.

#### 6.1.6 DEMC: Voltage

In most DMAS systems, a variable DC high-voltage supply is used to control the potential difference between the DEMC's electrodes. Fluctuations in the voltage across the DEMC will greatly affect the resulting particle size distribution measurement.

For large, low-mobility particles, the required voltage can be high, reaching up to 10 kV or 20 kV. The maximum voltage must be limited in order to prevent arcing within the instrument. Arcing generates artefact particles and can damage exposed surfaces in the instrument. The stability of the supplied voltage influences the resolution and repeatability of the DEMC.

For safety reasons, the outer DEMC surfaces are normally grounded while the variable, positive or negative voltage supply is connected to an inner electrode.

#### 6.1.7 DEMC: Temperature and pressure

The temperature and pressure inside the DEMC should be monitored during the measurement. Temperature and pressure fluctuations will adversely affect the data inversion unless they are taken into account.

**6.1.8 Particle detection: CPC**

Typically, a CPC has effectively 100 % counting efficiency over a wide range of particle sizes. Toward the low end of the detectable size range, the counting efficiency decreases to zero with a relatively steep sensitivity curve.

If the measuring range of the differential mobility analysing system extends into the range of the decreasing efficiency curve of the CPC, the measurements must be corrected accordingly.

A CPC must be operated within its specified particle concentration range. If the particle concentration is higher than the upper limit of the specified concentration range, particle coincidence will become significant and therefore will cause erroneous measurements.

**6.1.9 Particle detection: FCAE**

If an FCAE is used as a particle detector, the particle concentration exiting the DEMC shall provide an electrical current well above the noise level of the electrometer. Currently, aerosol electrometers measure electrical currents down to approximately 1 fA (or approximately 6 250 singly-charged particles per second).

**6.1.10 Data acquisition**

Most commercially available instruments have data acquisition software. It is important to make sure that the software collects all of the necessary data during the measurement. This will include the particle counts (from the particle counter) or electrical current (from the electrometer), the DEMC voltage, all necessary flow rates, temperature, pressure, etc. Some software packages have more options than others. Refer to the instrument manufacturer's manuals for details on setting up the data acquisition system.

**6.2 Pre-measurement checks**

**6.2.1 General**

There are several tests that can be made to ensure that the entire system is operating properly. These tests are also helpful in instrument troubleshooting.

**6.2.2 Overall DMAS check**

Apply clean air (through a HEPA filter) to the DMAS inlet and run a size distribution measurement. There should be no (or only very few) particles detected across the whole particle size distribution. Remove the filter to expose the DMAS to normal, non-filtered air and run another size distribution measurement. Check if a significantly larger number of particles are observed in the size distribution compared to that of filtered air.

**6.2.3 Data acquisition check**

Ensure that the data acquisition system is connected and operating properly. Verify that the voltages, particle counts, flow rates and other necessary data are recorded.

**6.3 Measurement**

Once the instrument has been set up and checked, measurement can begin. The parameters of the measurement will depend on the type of DEMC system used and the type of aerosol being measured. In all cases, determination of the particle size distribution requires measuring the number concentration of all particles exiting the DEMC at a given voltage. These have the same electrical mobility but can have different sizes due to possible multiple charges. Repeated measurements of the particle concentration at different voltages will provide a concentration versus electrical mobility curve that is the basis for determining the size distribution.

There are many different ways to run a DMAS. It is up to the operator to decide on the best method based on the measurements to be made, the equipment used and the instrument manufacturer's recommendations.

For the measurement, a few considerations should be noted.

- a) A stepping DEMC system changes the voltage between concentration measurements. For a stepping system, it is important to allow enough time for the particle detector to achieve a steady-state concentration. The amount of time needed for each step can be approximated by determining the travel time of the aerosol from the DEMC inlet to the particle detector based on the operating flow rate and tube length. Some commercial software packages can reduce the time needed between voltage steps by the use of proprietary algorithms. However, manual scans and manual adjustments will usually need longer times at each voltage.
- b) A scanning DEMC system smoothly changes the voltage (often as an exponential ramp) during a continuous measurement of the particle concentration. The scanning direction “upscan” designates a scan from a low voltage to a high voltage. The inverse is called “downscan”. For a scanning system, the time constants (residence time of the particle in the DEMC, residence time in the tubing between DEMC and particle detector, the response time of the particle detector and the time constant for the voltage ramp) and the scanning direction may cause a shift and a deformation of the transfer function compared with the stepping system (Collins *et al.*, 2004, [12]).
- c) It is important to know the stability of the source. Rapid changes of the size distribution, the particle concentration, or both, affect the measurement of the size distribution. Critical conditions of the particle source can be identified by repeating the size distribution measurement and by changing the measuring procedure (number of voltage steps, scan time).

The periodic tests and calibrations required during measurement are set out in Clause 7.

## 6.4 Maintenance

The maintenance schedule for a DEMC depends highly on the application, including aerosol type and aerosol concentration. The interval for maintenance depends on the sampled aerosol concentration and frequency of use. The following parts of a DEMC should be regularly cleaned:

**Inlet pre-separator:** Impactor nozzles should be cleaned with compressed air or an ultrasonic bath. Particles collected on an impactor plate should be removed and the plate should be recoated with a thin layer of vacuum grease. The maintenance should be done every six hours of sampling unless experience has proven that longer sampling times between cleanings may be tolerated.

**Neutralizer:** Radioactive sources should be checked to ensure the source has not exceeded its useful lifetime as indicated by an expiration date or date of manufacture. Cleaning such sources can be hazardous and should only be performed by a trained professional. The cleaning or repair of radioactive sources by the end-user is not recommended.

**Electrodes:** DEMC electrodes should be cleaned after every few months of continuous sampling. Use a very soft tissue to clean all electrode surfaces. Some particles on the electrodes will have no effect on the classification efficiency, but layers of particles could cause flow disturbances and could distort the electrical field. After cleaning, the surfaces of the DEMC electrodes should be checked visually for any damage. Even small scratches could lead to flow disturbances or change the electrical field, causing turbulence and resulting in an inaccurate transfer function for the DEMC.

**Other internal components:** During operation, many components are exposed to solid or liquid particle deposition. All components that are exposed to such deposition shall be cleaned regularly. Excessive soiling may change the geometry and particle cut-size of the preconditioner, may reduce the efficiency of the particle charge conditioner, may distort the electric field and/or the laminar flow in the DEMC and may affect the accuracy of the particle detector.

**Filters for sheath air/excess air:** Most of the aerosol particles entering a DEMC will not be classified and will exit with the excess air flow and deposit on a clean-air filter. The filter shall be replaced when necessary to avoid creating a large pressure drop within the sheath air flow, which is normally obtained from recirculation of the excess air flow.

## 7 Periodic tests and calibrations

### 7.1 Overview

Following the procedures below will ensure that a DMAS attains a known, small uncertainty for measurement of particle size and concentration. These procedures shall be performed only by qualified personnel. The procedures shall cover the fundamental components as summarized in the matrix.

**Table 3 — Matrix for sensitive components of a DMAS**

	Preconditioner	Particle charge conditioner	DEMC	Aerosol particle detector	System controller
Leak test	X	X	X	X	
Zero tests	X	X	X	X	
Flow meter calibration			X	X	X
Voltage calibration			X		X
Particle charge conditioner integrity test		X			
Calibration for size measurement	X	X	X	X	X
Size resolution test	X	X	X	X	X
Number concentration calibration				X	

### 7.2 Leak test

Each component shall be tested to ensure it is free of significant leaks. A significant leak is, for example, one that causes a change of greater than 5 % per hour in pressure inside the component during a vacuum leak test. The leakage rate measured during a leak test shall be recorded.

To check the leakage of air into or out of the DEMC, plug the sample inlet, sheath air inlet and the excess air connection of the DEMC. Connect a manometer to measure the pressure inside the DEMC. Connect a vacuum pump to the monodisperse aerosol outlet and excess air connections. Draw the pressure inside the DEMC down to less than 10 % of atmospheric pressure (< 10 kPa). Seal off the DEMC from the vacuum pump. Watch the pressure measured by the manometer for at least 1 hour. The DEMC leakage rate is acceptable if the pressure inside the DEMC measured by the manometer changes by less than 5 % per hour.

If the leakage test fails, the component shall be serviced to repair the leak.

NOTE 1 Testing some components for leaks, such as a CPC, requires special procedures that are specified by the manufacturer.

NOTE 2 If the excess air is recirculated to the sheath air, those two connections need not be plugged.

## 7.3 Zero tests

### 7.3.1 General

Once the flow rates are checked, there are three zero tests that can be performed to ensure that there are no leaks and that the instruments are working properly.

### 7.3.2 Particle detector zero test

Disconnect the particle detector from the DEMC and keep the tubing exposed to normal office or laboratory room air (not clean-room air). Ensure that the instrument is on and there is air flow into the particle detector at the correct rate. The particle detector should count a high concentration of particles. The particle detector may even saturate while sampling room air. Place a high-efficiency particulate air (HEPA) filter on the inlet and make sure that the particle detector signal drops to a negligible level compared to the concentration to be measured.

### 7.3.3 DEMC zero test

Reconnect the particle detector to the rest of the DMAS, apply clean air (through a HEPA filter with at least 99.99 % efficiency) to the DMAS inlet and run a size distribution measurement. There should be no (or only very few) particles detected across the whole particle size distribution. If the particle detector detects particles, there are leaks in the DMAS, either in the components or in the interconnecting tubes. To test leakage for each component, go back to 7.2.

### 7.3.4 Overall DMAS zero test

Make sure the aerosol inlet tube to the DEMC is open to normal room air (not clean-room air). Set up the appropriate sheath flow and aerosol flow rates within the DEMC and to the particle detector. Set the voltage applied to the DEMC to 0 volts. The particle detector should count no particles. If the particle detector detects particles:

- a) the sheath/aerosol ratio could be too low and particles are diffusing into the aerosol outlet of the DEMC. This can be corrected by decreasing the aerosol flow rate or increasing the sheath flow rate.
- b) the flow rates within the DEMC are too high and turbulent conditions exist. If this is the case, reduce the flow rates to return to laminar flow. Annex E describes a test for laminar flow for cylindrical DEMC.

## 7.4 Flow meter calibration

The flow meters indicating the volumetric flow rates of sheath air, excess air, incoming aerosol and outgoing classified sample aerosol shall be calibrated against a flow meter that is traceable to internationally accepted standards.

Volumetric flow rates govern the DEMC transfer function. If mass flow meters are used to measure or control flow rate, transformation from mass flow rate to volumetric flow rate is necessary.

**NOTE** When the excess air is circulated and used as the sheath air, one can assume that the incoming and sample aerosol flows are equivalent if the air leakage in the circulation circuit is verified to be negligible. In such cases, the flow meters need only be calibrated for the sheath air and the sample aerosol.

## 7.5 Voltage calibration

The voltage applied across the DEMC electrodes shall be calibrated against a voltmeter that is traceable to internationally accepted standards.

## 7.6 Particle charge conditioner integrity test

Aging of radioactive materials in the particle charge conditioner slowly reduces its charging efficiency. Because the charging efficiency is a function of particle size and concentration, the integrity of the conditioner shall be tested using particle sizes and concentrations similar to those to be measured.

The test requires two radioactive neutralizers. If the size distributions of nearly monodisperse aerosol are not significantly different using the first neutralizer alone, the second neutralizer alone and both neutralizers in series, they are both suitable for the measurement.

Other types of particle charge conditioners, such as unipolar chargers, should be in good operating condition according to the manufacturer's specifications.

## 7.7 Calibration for size measurement

### 7.7.1 General

This subclause describes a method to test sizing accuracy of the DMAS.

### 7.7.2 Purpose of calibration

The tests and calibrations described in 7.2 to 7.6 are necessary to check accuracy and integrity of individual components of the DMAS. However, they are not necessarily sufficient for verification of the accuracy of sizing by a DMAS as an entire system. Therefore, a particle size calibration shall be carried out to test for accuracy.

DMAS calibration with standard monodisperse particles of a certified size requires due attention with respect to

- a) the method of dispersing these particles in air, preferably with electro spraying,
- b) the concentration of the particle dispersion in the liquid that has to be dispersed, which must be sufficiently low to substantially avoid the aerosolization of particles other than singlet particles,
- c) the due removal of any non-volatile dissolved materials from the liquid other than the certified particles (remove surfactants and ionic species, etc.) prior to the aerosolization of the particles.

The following subclause provides a procedure for calibration that uses particle size standards. The procedure is performed with the standard DMAS sizing method and includes the data inversion and correction algorithms given by the manufacturer.

### 7.7.3 Calibration with standard DMAS sizing method

Aerosolize particles with a certified size,  $d_c$ , and measure the size distribution of them by the DMAS under test. Calculate the number-weighted mean diameter,  $\bar{d}$ , from the size distribution data. Repeat this 5 times and calculate the average of the mean diameters,  $\bar{\bar{d}}$ . Report the relative error,  $\varepsilon$ , between  $\bar{\bar{d}}$  and  $d_c$ .

The standard particles should have a small uncertainty for the certified size and a narrow size distribution. The relative standard uncertainty for the certified size should be equal to or less than 5 %, and the relative standard deviation of the distribution should be equal to or less than 20 % in diameter, whenever possible.

The arithmetic mean should be used for calculation of  $\bar{d}$ . For example, when the size distribution is presented as  $\frac{dN}{d \log d}$  versus  $d$ :

$$\bar{d} = \frac{\int d \cdot \frac{dN}{d \log d} \cdot d \log d}{\int \frac{dN}{d \log d} \cdot d \log d} \quad (6)$$

NOTE 1 The following equation can be used to calculate the relative error,  $\varepsilon$ :

$$\varepsilon = \frac{\bar{d} - d_c}{d_c} \cdot 100 \quad (7)$$

The tolerance value for the relative error,  $\varepsilon$ , shall be prescribed based on the purpose or requirements of the measurement in which the DMAS is used, the sizing capability of a specific DMAS and the magnitude of the size uncertainty of the standard particles used in the test.

NOTE 2 Annex F contains a procedure for a more detailed evaluation of DMAS sizing accuracy.

#### 7.7.4 Report for sizing accuracy calibration

The following information shall be included in the report:

- a) date of calibration;
- b) certified size ( $d_c$ ) and its standard uncertainty [ $u_c(d_c)$ ] of the standard particles and – if applicable – the corresponding electrical mobility ( $Z_c$ );
- c) DMAS settings, such as flow rates, voltage range, voltage scan rate, etc.;
- d) pressure and temperature in the DEMC during test;
- e) average of the mean diameters,  $\bar{d}$ , or mean electrical mobility,  $\bar{Z}$ ;
- f) relative error,  $\varepsilon$ .

#### 7.8 Size resolution test

Any disturbance or inhomogeneity of the flow field and/or the electrical field can distort and broaden the transfer function.

When a DMAS measures the size distribution of monodisperse or quasi-monodisperse particles using the approximation method described in Annex D.1, the obtained distribution is broader than the actual distribution. This can be exploited to extract the information about the width (resolution) of the transfer function.

The relative standard deviation of the measured distribution of certified particles,  $\sigma_d$ , at measured particle diameter  $d$ , shall be compared with the relative actual standard deviation,  $\sigma_c$ , of the standard particles of certified diameter  $d_c$ . This comparison shall consider the theoretical resolution defined by transfer function (see 4.4). Let  $\Delta Z/Z^*$  designate the relative width of the transfer function. For example, when the DEMC is operated with the sheath and excess air flows set equal and hence the transfer function is triangular, the following equation should be satisfied to a prescribed tolerance:

$$\frac{\sigma_d}{d} \approx \sqrt{\left(\frac{\sigma_c}{d_c}\right)^2 + \left(\frac{\kappa \cdot \Delta Z}{2\sqrt{6} \cdot Z^*}\right)^2} \quad (8)$$

where

$$\kappa = -\frac{Z}{d} \cdot \frac{d(d)}{dZ} = \frac{S_c}{2S_c - 1 + BC \exp[-C / Kn(d)]} \quad (9)$$

$S_c$ ,  $B$ ,  $C$  and  $Kn$  are as defined in 4.2. Note that this equation is only valid when broadening of the transfer function due to Brownian motion of the particles is expected to be negligible.

## 7.9 Number concentration calibration

The measurement of the particle number concentration shall be calibrated against an aerosol particle detector that is traceable to internationally accepted standards.

Techniques for checking the number concentration of the particle detector are given in Annex B.

## 8 Reporting of results

Results will always be reported as a part of the results of the broader experimental system. ISO 9276-1 may be helpful for determining how to present size distribution results.

The DMAS parameters to be recorded for each experiment, or set of experiments, shall include the following:

- a) date of analysis;
- b) unique identification of the analysis laboratory;
- c) operator's name;
- d) unique identification of the sample;
- e) identification of the type of instrument used, including manufacturer, model number (if any) and serial number or other unique identification;
- f) sampled flow rate of the gas containing the aerosol particles;
- g) sheath air flow rate;
- h) excess air flow rate;
- i) exit aerosol flow rate;
- j) pressure inside the DEMC during the experiment;
- k) date and leakage rate of the most recent leak test;
- l) temperature inside the DEMC during the experiment;
- m) method of calculation employed, including formulas used;
- n) observations of unusual events during the experiment.

## Annex A (informative)

### Particle charge conditioners and charge distributions

#### A.1 General

The function of the particle charge conditioner in a DMAS is to establish a known size-dependent charge distribution on the sampled aerosol prior to the size classification process in the DEMC.

The charge distribution achieved by the particle charge conditioner can either be the bipolar equilibrium charge distribution or a known, stable unipolar charge distribution.

#### A.2 Electrical charge neutralization

The operation of electrical charge neutralization is a form of particle charge conditioning used to convert aerosol particles from the uncertain charged condition into the certain equilibrium charge distribution. To achieve this, aerosol particles are exposed to a sufficiently high concentration of bipolar ions for an exposure time. This bipolar ion concentration can be produced either by radioactive ionization of air from radioactive sources or by corona discharge ionization.

##### A.2.1 Equilibrium charge distribution

###### A.2.1.1 General

In a gaseous medium containing aerosol particles and a sufficient concentration of bipolar ions, an equilibrium bipolar charge distribution will develop on the particles as a result of the random thermal motion of the ions and the collision between ions and aerosol particles.

###### A.2.1.2 Charge distribution function of particles

Under the steady-state conditions in the case of bipolar charging, the charge distribution function  $f_p(d)$  (charging probability) can be expressed as:

$$f_p(d) = \frac{C_{N,p}}{C_N} = \frac{\prod_{p=+1}^{+\infty} (\beta_{p-1}^+ / \beta_p^-)}{\Sigma}, \quad \text{if } p \geq +1 \quad (\text{A.1})$$

$$f_p(d) = \frac{C_{N,p}}{C_N} = \frac{\prod_{p=-1}^{+\infty} (\beta_{p+1}^- / \beta_p^+)}{\Sigma}, \quad \text{if } p \leq -1 \quad (\text{A.2})$$

$$f_p(d) = \frac{C_{N,0}}{C_N} = 1/\Sigma, \quad \text{if } p = 0 \quad (\text{A.3})$$

where

$$\Sigma = \sum_{p=+1}^{+\infty} \left\{ \prod_{p=+1}^{+\infty} \left( \beta_{p=+1}^+ / \beta_p^- \right) \right\} + \sum_{p=-1}^{-\infty} \left\{ \prod_{p=-1}^{-\infty} \left( \beta_{p=-1}^- / \beta_p^+ \right) \right\} + 1$$

$f_p(d)$  is the charge distribution as a function of particle size  $d$ ;

$C_N$  is the number concentration of aerosol particles of size  $d$ ;

$C_{N,p}$  is the number concentration of charged particles of particle size  $d$ ;

$C_{N,0}$  is the number concentration of uncharged particles of size  $d$ ;

$\beta$  is the ion-aerosol attachment coefficient of particles of size  $d$ ;

$p$  is the number of elementary units of charge.

From the above Equations (A.1), (A.2), (A.3), if the ion-aerosol attachment coefficients (combination charging constants)  $\beta$  corresponding to  $Z$  are known, the charge distribution function  $f_p(d)$  can be calculated and may be used in Equation (5) in the text.

### A.2.1.3 Ion-aerosol attachment coefficient — Fuchs' Theory

Under the steady-state charging processes, there is well-known expression about the ion-aerosol attachment coefficients,  $\beta$ , which is the so-called Fuchs' attachment theory, that can be expressed as:

$$\beta_p^\pm = \frac{\pi \cdot c^\pm \cdot \alpha \cdot \delta^2 \cdot \exp\{-\varphi(\delta)/kT\}}{1 + \exp\{-\varphi(\delta)/kT\} \frac{c^\pm \cdot \alpha \cdot \delta^2}{4D^\pm \cdot a} \int_0^{a/\delta} \exp\{\varphi(a/x)/kT\} dx} \quad (\text{A.4})$$

where

$$x = a/r$$

$$\varphi(r) = \int_0^\infty \Theta(r) \cdot dr = \frac{p \cdot e^2}{4\pi \cdot \epsilon_0 \cdot r} - \frac{\epsilon_1 - 1}{\epsilon_1 + 1} \frac{e^2}{8\pi \cdot \epsilon_0} \frac{a^2}{r^2 (r^2 - a^2)}$$

$$D^\pm = \frac{a^3}{\lambda^{\pm 2}} \left\{ \frac{1}{5} \left( 1 + \frac{\lambda^\pm}{a} \right)^5 - \frac{1}{3} \left( 1 + \frac{\lambda^{\pm 2}}{a^2} \right) \cdot \left( 1 + \frac{\lambda^\pm}{a} \right)^3 + \frac{2}{15} \left( 1 + \frac{\lambda^\pm}{a} \right)^{5/2} \right\}$$

$$\alpha = \left( \frac{a}{\delta} \right)^2$$

$a$  is the aerosol particle radius ( $d = 2a$ );

$r$  is the distance between the particle and the ion;

$c^\pm$  is the thermal velocity of positive or negative small ions;

- $\alpha$  is called Fuchs'  $\alpha$  parameter, corresponding to the square of the ratio of the particle radius to the limiting sphere;
- $\delta$  is the radius of a sphere that divides the free molecular regime near the particle and the continuum regime far from the particle; this imaginary sphere is often called Fuchs' limiting sphere;
- $k$  is the Boltzmann constant;
- $T$  is the absolute temperature;
- $D^\pm$  is the thermal diffusion coefficient of positive or negative small ions;
- $\varepsilon_0$  is the dielectric constant;
- $\varepsilon_1$  is the specific dielectric constant;
- $\lambda^\pm$  is the mean free path of positive or negative small ions.

If the values of dynamic properties  $c^\pm$ ,  $D^\pm$ ,  $\lambda^\pm$  of the small ion, and aerosol particle diameter  $d = 2a$  are known, the ion-aerosol attachment coefficients,  $\beta$ , can be calculated.

#### A.2.1.4 Properties of the ion

The values of dynamic properties  $c^\pm$ ,  $D^\pm$ ,  $\lambda^\pm$  of small ions can be defined from fundamental gas kinetic theories.

The relationship between the diffusion coefficient and mobility was given by Einstein (1905) [17]; it can be expressed as:

$$D^\pm = kTZ^\pm / e \quad (\text{A.5})$$

where  $Z^\pm$  is the electrical mobility of small ions.

The thermal velocity of small ions was derived by Kennard (1938) [32]; it can be expressed as:

$$c^\pm = \sqrt{\frac{8kT}{\pi \cdot m^\pm}} \quad (\text{A.6})$$

where  $m^\pm$  is the mass of a small ion.

There are several approximation methods for the mean free path of small ions. The representative example of these can respectively be expressed as:

$$\lambda^\pm = \frac{16\sqrt{2}}{3\pi} \cdot \frac{D^\pm}{c^\pm} \cdot \left( \frac{M}{M + m^\pm} \right)^{1/2}, \quad \text{described by Fuchs and Sutugin (1970) [21]} \quad (\text{A.7})$$

$$\lambda^\pm = \frac{32}{3\pi} \cdot \frac{D^\pm}{c^\pm} \cdot \left( \frac{M}{M + m^\pm} \right)^{1/2}, \quad \begin{array}{l} \text{a first-order Chapman-Enskog approximation,} \\ \text{explained by Bricard (1965) [8]} \end{array} \quad (\text{A.8})$$

$$\lambda^\pm = \frac{1}{1+\sigma} \cdot \frac{16\sqrt{2}}{3\pi} \cdot \frac{D^\pm}{c^\pm} \cdot \left( \frac{M}{M+m^\pm} \right)^{1/2}, \text{ described by Pui (1976) [44], Pui et al. (1988) [45], and}$$

Hoppel et al. (1986) [28] (A.9)

where

$M$  is the average molecular mass of air;

$\sigma$  is a correction factor:  $\sigma = 0,132$ .

If the ion properties  $Z^\pm$  and  $m^\pm$  are known, the charge distribution function,  $f_p(d)$ , can be calculated. The values of several ion properties are shown in Table A.1.

**Table A.1 — Values of ion properties used by various authors**

Mobility of ion		Mass of ion		Author and reference
$Z^+ (\times 10^{-4} \text{m}^2 \text{V}^{-1} \text{s}^{-1})$	$Z^- (\times 10^{-4} \text{m}^2 \text{V}^{-1} \text{s}^{-1})$	$m^+ (\text{amu})$	$m^- (\text{amu})$	
1,15	1,425	290	140	Reischl et al. (1996)
1,40	1,90	109	50	Adachi et al. (1985)
1,40	1,90	130	100	Adachi et al. (1985)
1,15	1,39	140	101	Porstendörfer et al. (1983)
1,20	1,35	150	90	Hoppel and Frick (1986)
1,15	1,39	140	101	Hussin et al. (1983)
1,35	1,60	148	130	Wiedensohler et al. (1986)
1,33	1,84	200	100	Hoppel and Frick (1990)
1,40	1,60	140	101	Wiedensohler and Fissan (1991)

**A.2.1.5 Approximation of the bipolar charge distribution for aerosol particles**

As described in above subclauses, an expert user of DMAS should be able to calculate the charge distribution function,  $f_p(d)$ . However, those calculation methods are long and complicated. Therefore, an empirical expression to approximate the charge distribution function,  $f_p(d)$ , in the size range from 1 nm to 1 000 nm is presented in this subclause. This approximation permits a useful and rapid calculation of the bipolar charge distribution function.

For an aerosol particle carrying up to two elementary charges, in charge equilibrium, the charge distribution function,  $f_p(d)$ , can be expressed using the approximation given in Equation (A.10), derived from the Fuchs model. To develop this approximation, specific values of ion properties are taken, and their sources are

- a) ion mobilities from Wiedensohler et al. (1986) [52],
- b) ion masses from Hussin et al. (1983) [30],
- c) the Fuchs'  $\alpha$  parameters from Hoppel and Frick (1986) [28] (see Table A.1).

The coefficients  $a_i(p)$  were determined using a least-square regression analysis and are listed in Table A.2.

$$\log[f_p(d)] = \sum_{i=0}^5 a_i(p) \cdot (\log d)^i \tag{A.10}$$

This equation is valid for the size range:

$$1 \text{ nm} \leq d \leq 1\,000 \text{ nm for } p = \{-1, 0, 1\} \text{ and}$$

$$20 \text{ nm} \leq d \leq 1\,000 \text{ nm for } p = -2, 2.$$

NOTE In this equation, *d* is in units of nanometres.

The charge distribution function,  $f_p(d)$ , with three or more elementary charge units can be calculated using the following Equation (A.11), which is based on Gunn's model:

$$f_p(d) = \frac{e}{\sqrt{4\pi^2 \epsilon_0 d k T}} \cdot \exp \left[ \frac{- \left[ p - \frac{2\pi \epsilon_0 d k T}{e^2} \cdot \ln \left( \frac{N_I^+ \cdot Z_i^+}{N_I^- \cdot Z_i^-} \right) \right]^2}{2 \frac{2\pi \epsilon_0 d k T}{e^2}} \right] \tag{A.11}$$

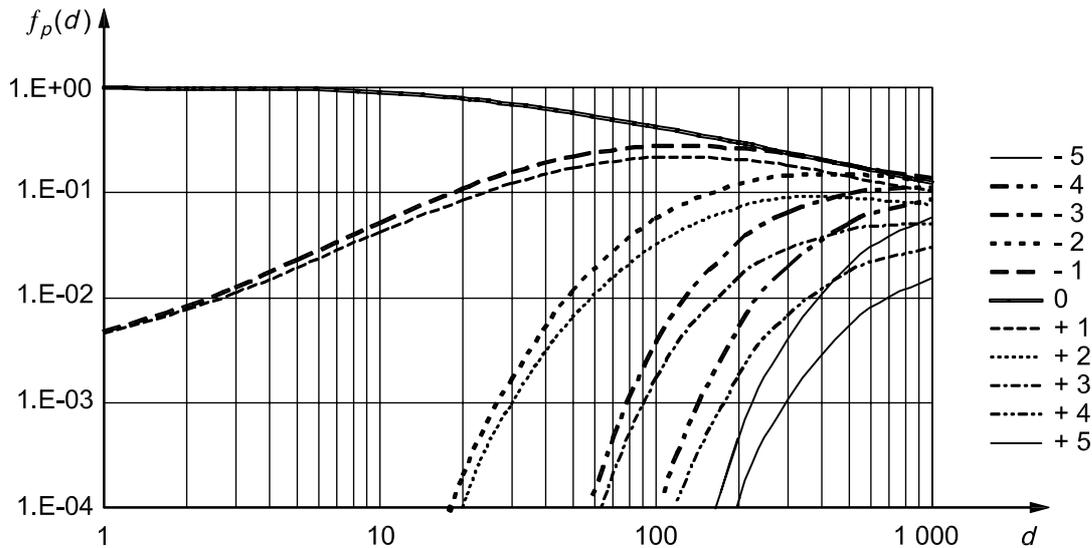
where

$N_I^\pm$  is the concentration of positive or negative small ions.

For this calculation, the concentration of positive and negative ions is assumed to be equal, and the ratio of ion mobilities  $Z_i^+ / Z_i^-$  was taken from Wiedensohler *et al.* (1986) to be 0,875. The results of this calculation are given in Figure A.1 below and in Table 2 in the text.

**Table A.2 — Coefficients  $a_i(p)$  for Equation (A.10)**

<i>i</i>	$a_i(p)$				
	$p = -2$	$p = -1$	$p = 0$	$p = +1$	$p = +2$
0	-26,332 8	-2,319 7	-0,000 3	-2,348 4	-44,475 6
1	35,904 4	0,617 5	-0,101 4	0,604 4	79,377 2
2	-21,460 8	0,620 1	0,307 3	0,480 0	-62,890 0
3	7,086 7	-0,110 5	-0,337 2	0,001 3	26,449 2
4	-1,308 8	-0,126 0	0,102 3	-0,155 3	-5,748 0
5	0,105 1	0,029 7	-0,010 5	0,032 0	0,504 9



**Key**

*d* particle diameter, expressed in nanometres  
*f<sub>p</sub>(d)* charging probability (-)

**Figure A.1 — Charging probability function for particles in the size range between 1 nm and 1 000 nm calculated from Equations (A.10) and (A.11)**

**A.2.2 *N<sub>I</sub>t* product**

The degree of neutralization mainly depends on the *N<sub>I</sub> · t* product, which is the concentration of bipolar ions, *N<sub>I</sub>*, multiplied by the residence time, *t*, of the aerosol particles in the ion cloud. For polydisperse aerosols (size range from 1 nm to 1 000 nm) passing through a particle charge conditioner, the *N<sub>I</sub> · t* product can be described as follows:

$$N_I^\pm \cdot t = -\frac{1}{\beta^\pm} \cdot \ln\left(1 - \frac{N_p^\pm}{N}\right) \tag{A.12}$$

This equation is derived from the subclause above (A.2.1.5). The ion-aerosol attachment coefficient, *β*, is strongly dependent on the aerosol particle diameter; it is in the order of 10<sup>-12</sup> m<sup>3</sup> s<sup>-1</sup>, therefore, the *N<sub>I</sub> · t* product has been found to be approximately 6 × 10<sup>12</sup> m<sup>-3</sup> s and 1 × 10<sup>12</sup> m<sup>-3</sup> s for the two limiting cases *Kn* << 1 and *Kn* >> 1, respectively. Therefore, a design-dependent upper particle concentration limit exists beyond which the charge equilibrium condition will not be reached. For an *N<sub>I</sub> · t* product larger than about 1 × 10<sup>13</sup> m<sup>-3</sup> s, the equilibrium charge distribution will be achieved in most practical situations.

The ion concentration is related to the intensity of the ion pair production rate. In particle free air, this intensity is expressed as:

$$i = \gamma \cdot N_I^+ \cdot N_I^- \tag{A.13}$$

where

- i* is the ion pair production rate;
- γ* is the recombination coefficient of positive and negative small ions.

If the effective volume,  $V$ , of the ionized area is known, the ion pair production rate,  $\iota$ , can be calculated from the measured saturation current,  $I$ , by the following equation:

$$\iota = \frac{I}{e \cdot V} \quad (\text{A.14})$$

To measure the ion pair production rate, the ionization source can be mounted on a polytetrafluoroethylene (PTFE) insulating support and inserted into a copper tube. With a DC voltage applied between the ionization source and the copper tube, the electrical charges can be measured as electric current using an electrometer.

### A.2.3 Ionization sources

There are two types of ionization sources for DMASs, based on radioisotopes and corona-discharges.

In the case of radioisotope methods, generally, a sealed radioactive source mounted in the neutralizer housing is used to achieve the equilibrium charge distribution. This device acts as a bipolar diffusion particle charge conditioner. It produces both negative and positive ions in the carrier gas. The radiation generates so-called primary ions like  $\text{N}_2^+$  and  $\text{O}_2^+$  and free electrons in the carrier gas. These ions are short-lived. Some of them attach themselves to neutral molecules, which then coagulate into relatively stable ion clusters. Diffusion (Brownian movement) leads to collisions between these ions and the aerosol particles and thus to charge transfer to the particles. The  $N_I \cdot t$  product reached in a radioactive neutralizer depends on the type and energy of the radiation of the isotope, on the activity and geometry of the sealed source, on the geometry of the housing, on the flow rate of the aerosol through the housing and on the carrier gas.

#### A.2.3.1 Radioisotopes

Most neutralizers are designed as stainless steel housings, which contain a sealed radioactive source. Krypton 85 ( $^{85}\text{Kr}$ ), americium 241 ( $^{241}\text{Am}$ ) and polonium 210 ( $^{210}\text{Po}$ ) are the most commonly used radioisotopes. These properties are explained in the following subclauses.

##### A.2.3.1.1 Krypton 85 ( $^{85}\text{Kr}$ )

$^{85}\text{Kr}$  is a beta emitter (with additional very low gamma radiation) with a half-life of 10,78 years. Its maximal beta energy is 0,695 MeV. Krypton is a noble gas, substantially reducing the health risk in case of leakage or damage to the source. After approximately 10 years,  $^{85}\text{Kr}$  sources should be replaced. In nearly all  $^{85}\text{Kr}$  neutralizers, the  $^{85}\text{Kr}$  gas is contained in a small-diameter sealed stainless steel tube. The small-diameter tube is contained inside a larger-diameter stainless steel or aluminium housing. Aerosol passes axially through the housing that contains the  $^{85}\text{Kr}$  tube. Part of the beta radiation is absorbed in the steel or aluminium that makes up the tube and the housing, thus producing Bremsstrahlung that also contributes to ion production. The activity for most DEMC applications ( $< 10^7$  particles  $\text{cm}^{-3}$  at sample air flow rates of  $< 0,5$  l/min) should be around 370 MBq (= 10 mCi).

##### A.2.3.1.2 Americium 241 ( $^{241}\text{Am}$ )

$^{241}\text{Am}$  is a solid alpha emitter (with additional very low beta and gamma radiation). Sealed sources are available as strips covered with a very thin gold film. The alpha energy is 5,6 MeV and it has a half-life of 433 years. The activity for most DEMC applications ( $< 10^7$  particles  $\text{cm}^{-3}$  at sample air flow rates of  $< 0,5$  l/min) should be approximately 5 to 10 MBq.

##### A.2.3.1.3 Polonium 210 ( $^{210}\text{Po}$ )

$^{210}\text{Po}$  is an alpha emitter. Its alpha energy is in the range between 4 MeV and 5,3 MeV and it has a half-life of 138 days. It is available in the form of gold-coated strips, typically embedded in a protective housing. The required activity for most DEMC applications ( $< 10^7$  particles  $\text{cm}^{-3}$  at sample air flow rates of  $< 0,5$  l/min) should be approximately 5 MBq to 10 MBq. Due to their short half-life,  $^{210}\text{Po}$  sources must be replaced annually or more often.

### A.2.3.2 Licensing and precautions for radioisotopes

The use, transportation and disposal of radioisotopes are regulated by government authorities. Basic international standards and guidelines are, for example, set by commissions of the United Nations like IAEA, ICRP, ADR, etc. The licensing, shipping and disposal regulations that govern radioactive sources vary from nation to nation. This International Standard can therefore only advise all users of radioactive material that local, national and international laws and regulations must be considered and followed.

### A.2.3.3 Corona discharge

Corona discharge may also function as a source for both negative and positive ions in the carrier gas. Either a single corona electrode operated with AC-high voltage or two separate corona electrodes (one for each ion polarity) can be used. If an aerosol electrometer is used as a particle detector, an ion trap may be necessary as an additional element to eliminate any remaining free ions from the charge-neutralized aerosol; otherwise an aerosol electrometer would measure these free ions as an additional current.

If corona discharge methods are used to achieve equilibrium charge distribution in the aerosol sample flow of a DMAS, the instrument manufacturer and the user shall, by design or by measurement, ensure that the method performs correctly and does not produce artefact particles.

## A.3 Unipolar electrical charging

Besides the widely used equilibrium charge distribution, unipolar electrical charging can also be used to achieve a defined charge distribution in a DMAS. In a unipolar charger, ions of either positive or negative polarity are produced by a corona discharge process. Like in bipolar charging, diffusion charging is advantageous because variations caused by the composition of the particles can be neglected for diffusion charging.

Unipolar electrical charging can achieve higher charging probabilities than bipolar charging. This is an advantage if small particles ( $d < 20$  nm) are to be measured. Due to the higher charging probability, more particles are classified by the DEMC and reach the particle detector. This leads to better counting statistics. On the other hand, larger particles ( $d > 100$  nm) carry significantly more multiple charges compared to bipolar charging. This makes the data inversion more complex and reduces the size resolution of large particles.

A variety of unipolar chargers for aerosol particles have been described and built; see, for example, Hewitt (1957), Medved *et al.* (2000), Büscher *et al.* (1994), Chen and Pui (1999) and Pui *et al.* (1988). Many of these chargers are used in combination with one or more aerosol electrometers as particle detectors. Some of these chargers have an ion trap as an additional element. The ion trap eliminates any remaining free ions from the charged aerosol; otherwise the aerosol electrometer will measure these free ions as an additional current.

If corona discharge methods are used to achieve a defined unipolar charge distribution in the aerosol sample flow of a DMAS, the instrument manufacturer and the user shall, by design or by measurement, ensure that the method performs correctly and does not produce artefact particles.

The particle concentration to be charged must be limited in such a way that the depletion of the ion concentration due to ion attachment to the particles does not lead to significantly reduced charges on the particles.

## Annex B (informative)

### Particle detectors

#### B.1 General

It is necessary to select an appropriate particle detector to measure particle concentration downstream of the DEMC. For this purpose, a condensation particle counter (CPC) or a Faraday-cup aerosol electrometer (FCAE) is generally used. These detectors are described below.

#### B.2 Condensation particle counter

##### B.2.1 General

Aerosol particles entering the CPC are first exposed to an atmosphere containing condensable supersaturated vapour in a component called a “saturator”. A supersaturated condition is generated, causing vapour to condense on the particles, growing the particles into droplets that can be detected by means of light scattered from a light beam.

Typically, a CPC has almost 100 % counting efficiency over a wide range of particle sizes larger than a defined minimum particle size. The counting efficiency decreases to zero at the minimum detectable particle size. To measure the particle size distribution using a CPC, it is necessary to correct the counting efficiency for particles in the size range in which a CPC has less than 100 % counting efficiency.

A CPC usually needs to cover a particle concentration range up to  $10^4$  or  $10^5$  particles per cubic centimetre. Because the droplet diameter in the detection zone of a CPC is usually several micrometres and the signal-to-noise ratio for single-droplet-counting is relatively high, a CPC is a reliable method to detect low concentration aerosols. The maximum concentration for single-droplet-counting is limited by the optical design of the instrument and is usually in the range of  $10^3$  to  $10^5$  particles per cubic centimetre. If the particle concentration exceeds the upper limit of the specified concentration range of the CPC, particle coincidence becomes significant and the reported concentration will be incorrect.

To measure higher concentrations, some CPCs include a photometric detection method that detects the intensity of the light scattered from all the particles in the sensing zone of the instrument at any given time. A CPC with photometric concentration measurement shall be calibrated periodically to ensure accurate measurements.

Before using the CPC, the user shall confirm that:

- a) the flow rate into the CPC is correct. (The flow rate directly influences the particle concentration indicated by a CPC.)
- b) there is sufficient working liquid in the CPC reservoir. (If sufficient working liquid is not present or if the working liquid contains too much water, condensation of the working liquid on the particle will be inhibited. The result will be an incorrect indication of particle concentration.)

##### B.2.2 Calibration

This International Standard does not attempt to describe a calibration method that links number concentration measurements traceably to international standards. The calibration described here is a comparison method to

compare the particle detector being used with a reference detector. The requirements of a reference detector are not defined here.

To calibrate a CPC, calibration particles having nearly mono-size shall be used. As an example, sodium chloride particles may be generated by evaporation of sodium chloride in a tube oven to produce a vapour, followed by rapid cooling of the vapour. The mean particle diameter may be adjusted by changing the flow rate of air (or nitrogen) through the tube oven and by changing the temperature of the tube oven. However, sodium chloride particles produced in this way do not have sufficient mono-size for calibration of CPCs. Use of a DEMC to size-classify the sodium chloride aerosol produces sufficient mono-sized particles. For generating particles larger than 50 nm in diameter, a serial, tandem DEMC system is recommended to remove multiply-charged particles with sizes larger than desired that have the same electrical mobility as the desired singly-charged particles.

A pre-calibrated aerosol electrometer or CPC is used as a transfer standard. Details of an aerosol electrometer are described in B.3. A schematic diagram of the calibration system is shown in Figure B.1.

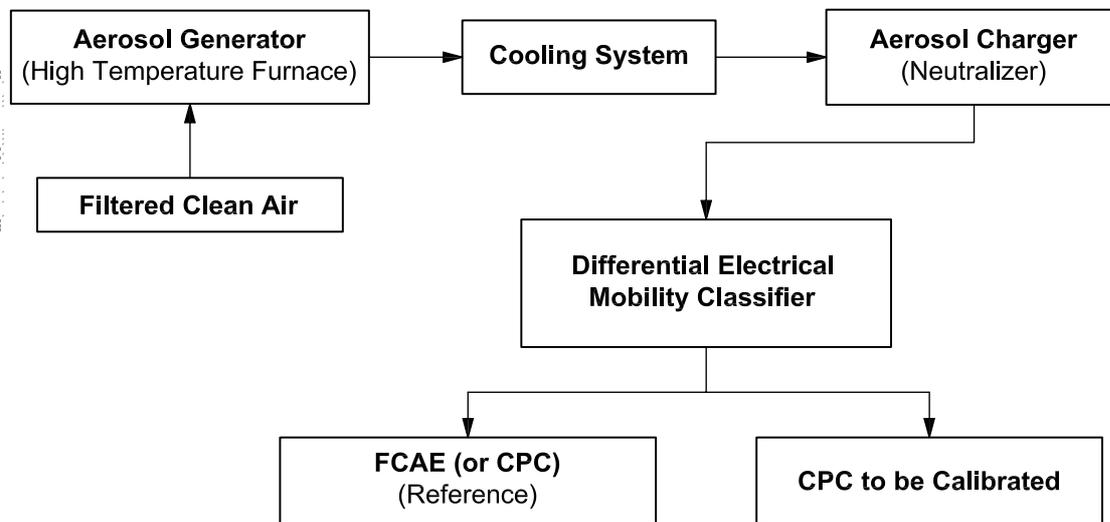


Figure B.1 — Example system component diagram for calibration of a CPC

To calibrate a CPC, its indicated concentration is compared to a pre-calibrated reference detector. This procedure is repeated for a range of particle sizes and number concentrations, such that the operating ranges of the detector are covered. The counting efficiency is defined by the following equation:

$$\text{Counting efficiency (\%)} = (\text{CPC indicated concentration} / \text{reference concentration}) \times 100 \tag{B.1}$$

The minimum particle detection size of a CPC is defined by the size having 50 % counting efficiency.

### B.3 Faraday-cup electrometer

#### B.3.1 General

An FCAE is a detector of the electrical current resulting from the collection of ions and charged particles in the sample flow. An FCAE is intended to operate in the pressure range between a few atmospheres and high vacuum. An FCAE captures both positive and negative electrical charges and reports the net charge. An FCAE measures the very low electrical current after the charge is released from the particles as they come in contact with conducting parts of the FCAE. When an FCAE is used as an aerosol detector with a DEMC, it must be designed to allow the gas to permeate through the filter and to fully capture the charged particles. Therefore, it is necessary for an FCAE to have a filter portion inside a cup-shaped housing to efficiently capture the electrical charges. It is not necessary for the filter to be made from conducting material, since

space charge on the collected particles will force the electrical current to the conducting surfaces of the Faraday cup that surrounds the filter.

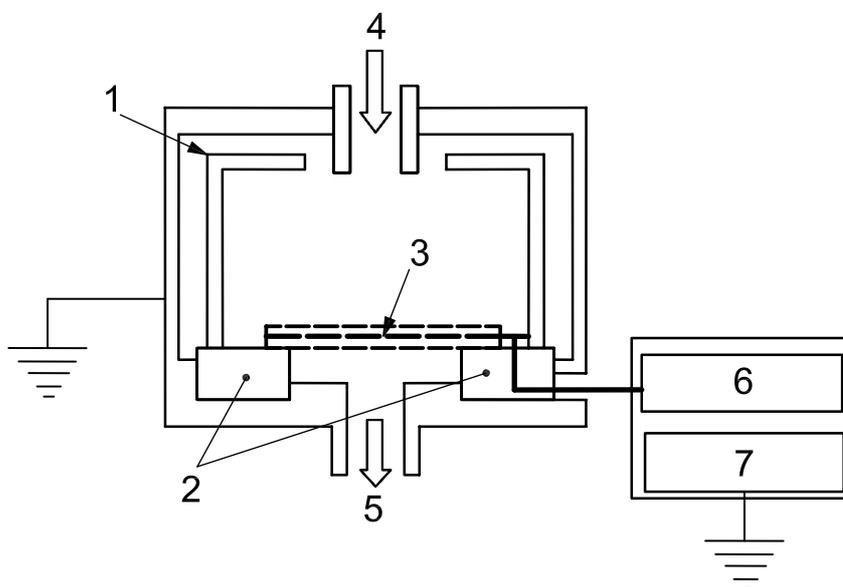
An FCAE is usually suited for the measurement of a charged particle number concentration in the range from  $10^4$  to  $10^8$  particles per cubic centimetre. If the electrical charging is based on equilibrium charging, the number concentration of the total (namely, positive, negative and neutral) fine particles in the actual sample gas is typically one to three orders-of-magnitude higher than the number concentration of the (positively or negatively) charged particles measured downstream of a DEMC, depending on the method of charging and the size distribution of the particles. Since the charging efficiency of fine particles depends on particle size, it is necessary to consider in advance whether the relevant sample particle number concentration is within the range of FCAE measurement. If measurements at a lower particle number concentration are necessary, one must consider use of a CPC detector as described in B.2.

While an FCAE being used as a detector with a DEMC is usually operated at or near atmospheric pressure, an FCAE may also be operated at low pressures, in an extreme case, as low as 200 Pa to 930 Pa. For low pressure operation, a special design is needed to reduce aerodynamic resistance.

### B.3.2 Structure and detection mechanism of FCAE

Figure B.2 shows a typical FCAE structure. When sample gas containing charged fine particles enters the inlet tube to the FCAE, the gas flows through the filter and the particles are collected on the filter. The filter is normally surrounded by a porous metallic housing, converting the filter into an ion collector. The charge on the fine particles is then released from the particles and forced by space charge within the filter material to the surrounding metal housing.

The electrical current thus formed is very minute, usually measured in units of femtoamperes. The current from the filter passes into an electrometer and is amplified. The amplified current is proportional to the particle number concentration, the average number of electrical charges per particle and the sample flow rate of the charged aerosol entering the FCAE.



#### Key

- 1 Faraday cup to collect electrical current from charged collected particles and to reduce externally-induced electro-magnetic noise
- 2 very-high-resistance electrical insulator to isolate the filter from electrical ground
- 3 high-efficiency particulate air (HEPA) filter to trap airborne charged particles
- 4 charged particles in
- 5 particle-free air out
- 6 preamplifier
- 7 electrometer

Figure B.2 — Schematic diagram of Faraday-cup aerosol electrometer (FCAE)

### B.3.3 Calibration

This subclause describes those elements within the FCAE that are to be calibrated during normal operation. It does not describe a calibration method that links FCAE number concentration measurements traceably to international standards.

If the filter in an FCAE is a HEPA filter, the efficiency of capturing the charge carried on airborne particles in a sample gas for the FCAE is very close to 100 %. Most electrometers contain a feedback resistor with very high resistance, typically  $10^{11} \Omega$  or  $10^{12} \Omega$ . The resistance of FCAE feedback resistors and the gain of the amplifier shall be calibrated annually. Since the resistance and gain directly affect the measured current of the electrometer, these values shall be maintained within 5 % of their nominal values.

The flow rate of sample through the FCAE directly affects the measured concentration. Therefore, the flowmeter used to measure the sample flow rate through the FCAE shall be calibrated at least annually.

An FCAE can also be calibrated by comparison to a pre-calibrated reference detector.

22

## Annex C (informative)

### Slip correction factor

#### C.1 General

The electrical mobility of a particle depends on the particle size and the number of elementary charges. A unique relationship between electrical mobility and particle size is described in 4.2. The theoretical expression for the drag force on a spherical particle moving with low Reynolds number in a gas phase is customarily written by multiplying the Stokes' law expression by a slip correction factor of the form given in Equation (2), repeated here as Equation (C.1), as introduced by Knudsen and Weber (1911).

$$S_c = 1 + Kn \left[ A + B \exp\left(-\frac{C}{Kn}\right) \right] \quad (\text{C.1})$$

where

$Kn = \frac{2l}{d}$  is the particle Knudsen number;

$l$  is the mean free path of gas molecule;

$d$  is the spherical particle diameter;

$A$ ,  $B$  and  $C$  are empirical constants;

$S_c$  is the slip correction.

The goal of this annex is to provide further detail on the source of the recommended parameters for the slip correction factor given in Table C.1.

#### C.2 Historical investigation of the slip correction factor

Table C.1 summarizes a number of measurements of slip correction parameters. Millikan's experiments were performed between 1909 and 1923 (Millikan 1910 [40], 1923 [41]). His last experiment extended the measurements up to  $Kn \sim 134$  and visually fitted his data using the form of Equation (C.1). Millikan used the well-known apparatus called "Millikan's oil droplet apparatus" or "Millikan's cell apparatus". He obtained values of  $A = 0,864$  and  $A + B = 1,154$ . He found that the value  $C = 1,25$  fitted his data from  $Kn = 0,25$  to 134. The earliest values for  $A$ ,  $B$  and  $C$  were determined by Knudsen and Weber (1911) [34] from the damping of torsional oscillation of a pair of glass spheres suspended in a vessel at low pressures; they obtained the values of 0,772, 0,40 and 1,63, respectively. Several authors have used Millikan's values for  $A$ ,  $B$  and  $C$  and have modified them using different values of the molecular mean free path,  $l$ , as shown in Table C.1. Fuchs recalculated a value of  $l = 65,3$  nm and modified Millikan's values to  $A = 1,246$ ,  $B = 0,42$  and  $C = 0,87$  (Fuchs, 1964) [20]. This set of values is probably the most widely used to correct Stokes' law.

Allen and Raabe (1982) [5] reviewed and re-evaluated Millikan's data using up-to-date values of the relevant physical constants and nonlinear least-squares function fitting to make new estimates of the three slip correction parameters:  $A = 1,155$ ,  $B = 0,471$  and  $C = 0,596$ . Also, they made slip correction measurements on solid spherical particles in air using Millikan's cell apparatus, and they obtained  $A = 1,142$ ,  $B = 0,558$  and  $C = 0,999$  (Allen and Raabe, 1985 [6]). They took the value of the mean free path,  $l$ , of air molecules at

$T_0 = 296,15$  K and  $P = 760$  mmHg to be  $6,73 \times 10^{-8}$  m. The mean free path for other temperatures  $T$  and pressures  $P$  was calculated using Equation (4).

They made a choice for the value  $\eta_0 = 1,8324 \times 10^{-5}$  kg m<sup>-1</sup> s<sup>-1</sup> for the viscosity of dry air at  $T_0 = 296,15$  K. The values of  $\eta$  for other temperatures were calculated using Equation (3).

The data from Millikan's cell experiments consist of a set of time intervals required for test particles to move vertically between two scale marks as determined visually by the operator. Millikan's cell method requires independent knowledge of the particle mass density, the absence of thermal air currents in the test cell, and detailed knowledge of the electric field in the test cell. For this reason, Hutchins, Harper and Felder (1995) [31] have measured slip correction factors for spherical solid particles in air with an automated apparatus using a new approach which requires none of Millikan's cell conditions. They emphasized that the new method was an application of the modulated dynamic light scattering method, which is fundamentally different from Millikan's cell, and that drag forces on spherical polystyrene latex particles were measured in dry air. In this method, the data are time autocorrelation functions of the intensity of light scattered by single particles from the intersection volume of two coherent laser beams.

This experiment provided detailed information about test particle Brownian motion, including the value of the particle diffusion coefficient. Each test was made on 72 solid spherical particles with diameters ranging from 1,0  $\mu\text{m}$  to 2,2  $\mu\text{m}$ , at air pressures ranging from 760 mmHg to 0,2 mmHg. Collected data provided 1 586 distinct experimental values of the slip correction factor with  $Kn$  ranging from 0,06 to 500. Analysis of these data gave the values  $A = 1,231 0 \pm 0,002 2$ ,  $B = 0,469 5 \pm 0,003 7$  and  $C = 1,178 3 \pm 0,009 1$  using the same equations of Allen and Raabe's analysis, where the mean free path of air molecules and the viscosity of dry air were taken to be  $6,73 \times 10^{-8}$  m and  $1,832 5 \times 10^{-5}$  kg m<sup>-1</sup> s<sup>-1</sup>, respectively, at 760 mmHg and  $T_0 = 296,15$  K. When they compared the results for the drag force ratio of solid and liquid particles, they indicated that the results from kinetic theory and from Allen and Raabe's re-evaluation of Millikan's data agree closely, and the results for solid particles from their work agree closely with Allen and Raabe's results for solid particles, but the kinetic theory and the drag force ratio values of oil droplets fall below those for solid particles over the range  $Kn = 0,09$  to 18, with differences as great as 8 %.

The most recent work was published by Kim *et al.* (2005) [33]. Based on the viscosity and mean free path of air molecules chosen by Allen and Raabe, they measured slip corrections using certified polystyrene latex (PSL) particles of precisely known size and a DEMC. The measurements covered a wide range of sizes (19,9 nm to 269 nm), pressures (98,5 kPa to 8,27 kPa) and Knudsen numbers (0,5 to 83). A detailed uncertainty analysis showed approximation uncertainties (95 % confidence interval) smaller than 3 % for the whole data set.

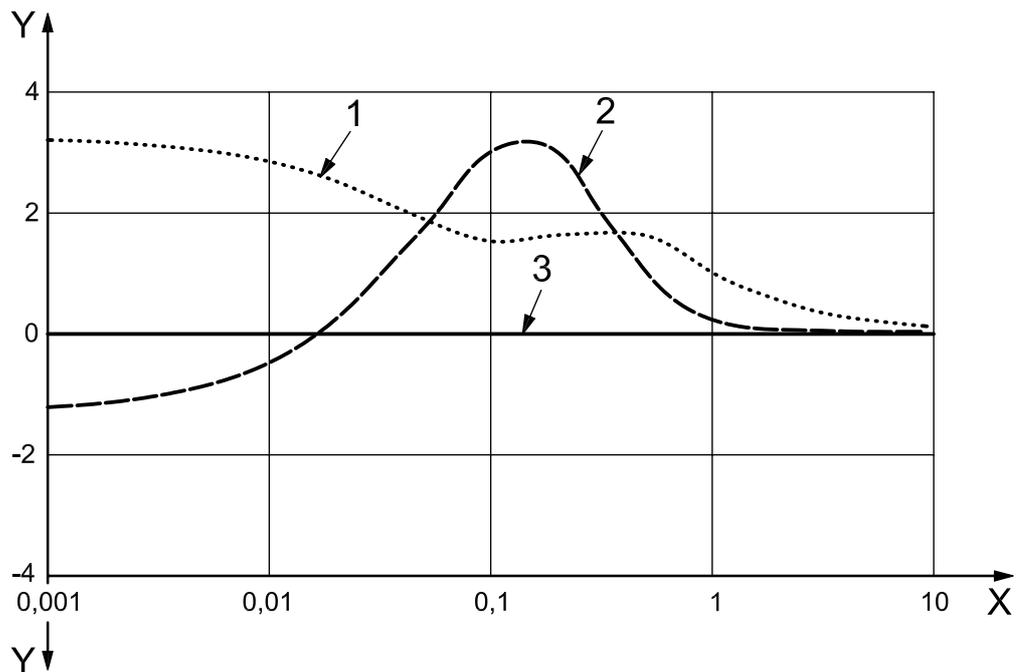
Table C.1 — Published values of slip correction factors for Stokes' law

Author	Mean free path $l$ ( $\mu\text{m}$ )	$A$	$B$	$C$	$A + B$	Bibliography and comments
Knudsen and Weber (1911)	0,094 17	0,772	0,400	1,630	1,172	Allen and Raabe (1982)
Millikan (1923b)	0,094 17	0,864	0,290	1,250	1,154	ibid.
Davies (1945)	0,066 0	1,257	0,400	1,100	1,657	ibid.
DeMarcus, Thomas (1952)	0,065 5	1,250	0,440	1,090	1,690	ibid.
Reif (1958)	0,065 2	1,260	0,450	1,080	1,710	ibid.
Dahneke (1973)	0,066 0	1,234	0,414	0,870	1,648	ibid.
Allen and Raabe (1982)	0,067 3	1,155	0,471	0,596	1,626	ibid., for liquid particles
Allen and Raabe (1985)	0,067 3	1,142	0,558	0,999	1,700	for solid particles
Hutchins, <i>et al.</i> (1995)	0,067 3	1,231	0,469 5	1,178 3	1,700 5	for solid particles
Millikan (1923b)	0,067 4	1,209	0,406	0,893	1,615	Rader (1990)
Rader (1990)	0,067 4	1,207	0,440	0,780	1,647	ibid.
Millikan (1923b)	0,094 17	0,864	0,290	1,250	1,154	Fuchs (1964)
Mattauch (1925)		0,898	0,312	2,370		ibid.
Fuchs (1964)	0,065 3	1,246	0,420	0,870	1,666	ibid.
Schmitt (1959)		1,45	0,40	0,9		ibid.
Kim, Mulholland, Kukuck and Pui (2005)	0,067 3	1,165	0,483	0,997	1,648	Measured with NIST certified PSL particles

### C.3 Recommended coefficients for the slip correction factor

In the above description, there is strong evidence that the results of Hutchins, Harper and Felder (1995) <sup>[31]</sup> of drag force ratio for solid particles closely agree with the results of Allen and Raabe (1985) <sup>[6]</sup> for solid particles and that the results for the drag force ratio from kinetic theory agree closely with Allen and Raabe's results from re-evaluation of Millikan's oil droplet data. However, the solid particle results differ from the kinetic theory and oil droplet results by up to 8 % in the Knudsen number range of 0,09 to 18.

Considering the traceability of the experiments, this International Standard recommends the use of the coefficients determined by Kim *et al.* (2005) <sup>[33]</sup> for particle size distribution measurements (as given in 4.2). Figure C.1 shows a comparison between the slip correction calculated with the coefficients by Hutchins, Harper and Felder (1995), Allen and Raabe (1985) and Kim *et al.* (2005). As can be seen, the relative difference of the first two calculations to the calculation with the recommended coefficients is within +3 % and -1 % over a particle diameter range from 1 nm to 10  $\mu\text{m}$ .



**Key**

- X particle diameter ( $\mu\text{m}$ )
- Y relative difference (%)
- 1 Hutchins *et al.* (1995)
- 2 Allen and Raabe (1985)
- 3 Kim *et al.* (2005)

**Figure C.1 — Slip correction and relative difference for coefficients from Hutchins *et al.* (1995) and Allen and Raabe (1985) compared to Kim *et al.* (2005)**

## Annex D (informative)

### Data inversion

#### D.1 General

Since the DEMC is generally operated at high resolution, non-zero values of the transfer function  $\Omega$  occur only in a narrow range of  $Z$ . Therefore, it is a common practice that, to solve Equation (5) for  $n(d)$ , the terms  $n(d)$ ,  $f_p(d)$  and  $W(d, p)$  are assumed to be constant within the non-zero interval of the transfer function  $\Omega$  and taken out of the integral as:

$$R(U) = q_2 \sum_{p=1}^{\infty} n(d_p^*) \cdot f_p(d_p^*) \cdot W(d_p^*, p) \int_{d=0}^{\infty} \Omega[Z(d, p), \Delta\Phi(U)] dd \quad (\text{D.1})$$

where  $d_p^*$  is the diameter of particles of charge  $p$  that has the electrical mobility equal to  $Z^*$ , which is the central electrical mobility of the transfer function for the set voltage  $U$  as given in 4.5.

**NOTE** When a DMAS measures the size distribution of monodisperse or quasi-monodisperse particles and the above approximation method is used in data inversion, the obtained distribution is broader than the actual distribution.

The integral in Equation (D.1) is further converted to:

$$\int_{d=0}^{\infty} \Omega[Z(d, p), \Delta\Phi(U)] dd = (dd/dZ)_{d_p^*} \int_{d=\infty}^0 \Omega(Z, Z^*) dZ \quad (\text{D.2})$$

The differential term  $dd/dZ$  is given in Clause F.4. The integral term corresponds to the area under the transfer function, which has a shape of either triangle or trapezoid as shown in Subclause 4.4.

There are several data inversion methods to solve Equation (D.1) while deconvoluting with respect to charge number  $p$ . The representative methods of Hoppel and Knutson are described below.

#### D.2 Hoppel method

In order to convert the mobility distribution to the size distribution, it is necessary to establish firstly the relationship between the mobility of a charged aerosol particle and its diameter and secondly the fraction of aerosol particles of a given size that carry a given number,  $p$ , of elementary charges. Since atmospheric aerosol particles cover a range from those that have radii much larger than the molecular mean free path to those that have radii smaller than the mean free path, it is impossible to relate the particle mobility to the particle size by using a single theory. This International Standard deals with three particle size ranges:

- first is the transitional regime ranging from 3,0 nm to 30,0 nm;
- second is the multiply-charged regime ranging from 30,0 nm to 300 nm;
- third is Junge's distribution regime ranging from 300 nm to 1 000 nm.

The relationship between electrical mobility and radius of an airborne particle is given by Equation (1) above. For an ionized aerosol in charge equilibrium as well as thermal equilibrium, we may assume that the Boltzmann distribution describes the number of electrical charges carried by aerosol particles. This results in a charge distribution on multiply-charged and Junge's distribution regime aerosols of radius  $r$  given by:

$$C_{N,p}(r) = C_{N,0}(r) \exp\left(-\frac{p^2 e^2}{2kTr}\right) \quad (D.3)$$

where

$C_{N,0}(r)$  is the number concentration of uncharged particles;

$C_{N,p}(r)$  is the number concentration carrying  $p$  elementary charges of one polarity;

$k$  is Boltzmann's constant;

$p$  is the number of elementary charges on the particle;

$e$  is the elementary charge;

$T$  is the absolute temperature.

For the transition regime, the number concentration of multiply-charged particles is negligible and the conversion of the mobility distribution to the size distribution shall use Equation (D.3), without any correction for multiply-charged particles.

For the multiply-charged and Junge distribution regimes, the total number concentration of aerosols of radius  $r$  irrespective of the charge level or charge polarity is denoted by:

$$X(r) = C_{N,0}(r) + 2 \sum_{p=1}^{\infty} C_{N,p}(r) \quad (D.4)$$

Combining Equations (D.3) and (D.4) yields the relationship between the total number of particles of radius  $r$  and the number with  $p$  elementary charges of one sign:

$$X(r) = \frac{C_{N,p}(r)}{R_p(r)} \left[ 1 + 2 \sum_{p=1}^{\infty} R_p(r) \right] \quad (D.5)$$

where

$$R_p(r) = \exp\left(-\frac{p^2 e^2}{2kTr}\right) \quad (D.6)$$

In the DEMC, only those aerosol particles that are charged can be detected. Charged particles in a specified mobility range  $(Z_{j+1} - Z_j)$  may be singly-charged particles of that mobility or multiply-charged particles that would be in a lower mobility range if they were singly-charged. Multiply-charged particles carrying  $p$  elementary charges would be in a reduced mobility range between  $Z_{j+1}/p$  and  $Z_j/p$  if they carried a single charge. In terms of their reduced single-charge mobility, the number of charged particles in the mobility range  $(Z_{j+1} - Z_j)$  can be written as:

$$\Delta N(Z_{j+1} - Z_j) = \Delta N_1(Z_{j+1} - Z_j) + \Delta N_2\left(\frac{Z_{j+1}}{2} - \frac{Z_j}{2}\right) + \dots + \Delta N_p\left(\frac{Z_{j+1}}{p} - \frac{Z_j}{p}\right) \quad (D.7)$$

In Equation (D.7),  $\Delta N_p \left[ r \left( \frac{Z_{j+1}}{p} \right) - r \left( \frac{Z_j}{p} \right) \right]$  is the number of particles with  $p$  elementary charges in the mobility range  $\left( \frac{Z_{j+1}}{p} - \frac{Z_j}{p} \right)$ . These particles are characterized by an equivalent single-charge mobility range  $\left[ \left( \frac{Z_{j+1}}{p} \right) - \left( \frac{Z_j}{p} \right) \right]$ . Denoting the functional dependence of the radius on the single-charge mobility as  $r(Z)$ , Equation (D.7) can be expressed as:

$$\begin{aligned} \Delta N \left[ r \left( Z_{j+1} \right) - r \left( Z_j \right) \right] &= \Delta N_1 \left[ r \left( Z_{j+1} \right) - r \left( Z_j \right) \right] + \Delta N_2 \left[ r \left( \frac{Z_{j+1}}{2} \right) - r \left( \frac{Z_j}{2} \right) \right] + \\ &\dots + \Delta N_p \left[ r \left( \frac{Z_{j+1}}{p} \right) - r \left( \frac{Z_j}{p} \right) \right] \end{aligned} \quad (D.8)$$

Equation (D.8) has been written to emphasize the fact that the mobilities of charged particles come from several size ranges that are different from singly-charged aerosols.

$\Delta N \left[ r \left( Z_{j+1} \right) - r \left( Z_j \right) \right]$  is readily obtained from experimentally-determined values of  $f(Z)$  (e.g.  $\Delta N = f(Z) \Delta Z$ ) obtained with a DEMC. From a set of measurements of  $\Delta N \left[ r \left( Z_{j+1} \right) - r \left( Z_j \right) \right]$  covering the entire mobility range, the number of aerosol particles in the size interval  $\left[ r \left( Z_{j+1} \right) - r \left( Z_j \right) \right]$ ,  $\Delta X \left[ r \left( Z_{j+1} \right) - r \left( Z_j \right) \right]$ , is calculated by the following method. Since there are nearly always more singly-charged particles than any other charge class (excluding zero charge) for the practical range of a DEMC, the first approximation assumes that all charged particles in the mobility interval are singly-charged. Equation (D.8) then becomes:

$$\Delta^{(1)} N_1 \left[ r \left( Z_{j+1} \right) - r \left( Z_j \right) \right] = \Delta N \left[ r \left( Z_{j+1} \right) - r \left( Z_j \right) \right] \quad (D.9)$$

where the numerical superscript denotes a first-order approximation. The first-order size distribution is then obtained from Equation (D.9) by calculating  $\Delta^{(1)} X$  for each mobility interval:

$$\Delta^{(2)} X \left[ r \left( Z_{j+1} \right) - r \left( Z_j \right) \right] = \left[ \left( 1 + 2 \sum_{p=1}^{\infty} R_p \left( \bar{r}_j \right) \right) / R_1 \left( \bar{r}_j \right) \right] \Delta^{(1)} N_1 \left[ r \left( Z_{j+1} \right) - r \left( Z_j \right) \right] \quad (D.10)$$

where  $\bar{r}_j$  is the size corresponding to the average mobility of the  $\left( Z_{j+1} - Z_j \right)$  interval. This approximation, of course, overestimates  $\Delta X$  because it attributes more singly-charged particles to the interval than are actually there.

The second approximation for calculating the number of singly-charged particles is derived from Equation (D.9) as:

$$\begin{aligned} \Delta^{(2)} N_1 \left[ r \left( Z_{j+1} \right) - r \left( Z_j \right) \right] &= \Delta N \left[ r \left( Z_{j+1} \right) - r \left( Z_j \right) \right] - \Delta^{(1)} N_2 \left[ r \left( \frac{Z_{j+1}}{2} \right) - r \left( \frac{Z_j}{2} \right) \right] + \\ &\dots - \Delta^{(1)} N_p \left[ r \left( \frac{Z_{j+1}}{p} \right) - r \left( \frac{Z_j}{p} \right) \right] \end{aligned} \quad (D.11)$$

where  $\Delta^{(1)} N_p$  is the number of multiply-charged particles estimated from Equation (D.8) using the first order approximation:

$$\Delta^{(1)} N_p \left[ r \left( \frac{Z_{j+1}}{p} \right) - r \left( \frac{Z_j}{p} \right) \right] = \left[ R_p \left( \bar{r}_j \right) / \left( 1 + 2 \sum_{p=1}^{\infty} R_p \left( \bar{r}_j \right) \right) \right] \Delta^{(1)} X \left[ r \left( Z_{j+1} \right) - r \left( Z_j \right) \right] \quad (D.12)$$

Equation (D.11) estimates the number of multiply-charged particles from larger size channels that are contributing to the charged particles observed in the mobility channel  $(Z_{j+1} - Z_j)$  and subtracts the multiply-charged particles to give a new estimate of the singly-charged particles in that channel. The new estimate of singly-charged particles  $(\Delta^{(2)}N_1)$  is then used to calculate the second approximation to the size distribution, given by the equation:

$$\Delta^{(2)}X[r(Z_{j+1}) - r(Z_j)] = \left[ \left( 1 + 2 \sum_{p=1}^{\infty} R_p(\bar{r}_j) \right) / R_1(\bar{r}_j) \right] \Delta^{(2)}N_1[r(Z_{j+1}) - r(Z_j)] \quad (D.13)$$

For higher approximations, the process given in Equations (D.10), (D.11) and (D.12) is repeated using the newly found approximation for  $\Delta X$ .

NOTE The procedure in this clause was reported by Hoppel (1978) [27].

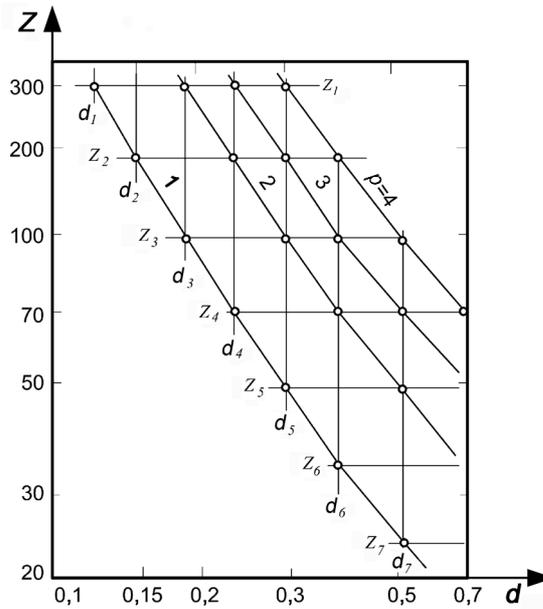
### D.3 Knutson method

This procedure was proposed by Knutson as a simple method of obtaining the particle size distribution. He used this method to measure atmospheric aerosols and laboratory-generated aerosols.

Firstly, the data inversion process is shown in Figure D.1.

The oblique lines mean the relationship between the electrical mobility and the particle diameter having  $p$  elementary charges. The mobility  $Z_j$ , shown as a vertical axis, is the electrical mobility to be obtained, and is set to have a ratio of 1,429 to the adjacent one. As already known, the classified particles at some voltage of DEMC include several groups of particles having different sizes, each group carrying a different number of elementary charges. For example, in case of  $Z_1$ , there are four different diameters of particles, 0,120  $\mu\text{m}$ , 0,186  $\mu\text{m}$ , 0,240  $\mu\text{m}$  and 0,292  $\mu\text{m}$ , corresponding to  $d_1$ ,  $d_2$ ,  $d_3$  and  $d_4$ , and they carry  $p = 1, 2, 3$  and  $4$  electrical charges, respectively. Generally speaking, classified particles having a mobility of  $Z_j$  consist completely of particles within the particle diameters of  $d_{i+1}$ ,  $d_{i+2}$ ,  $d_{i+3}$  and  $d_{i+4}$ , respectively.

.....



**Key**

- Z electrical mobility, expressed in cm<sup>2</sup>/volt-sec
- d particle diameter, expressed in micrometres
- p number of electrical charges carried by each particle

**Figure D.1 — Relationship between electrical mobility *Z* and particle diameter, *d***

Knutson assumed that the number of charges was no more than 4 and found the number concentration,  $C_{N,j}$ , by the following equation:

$$R_i = q_a \sum W_{p,j} \cdot \Phi_{p,j} \cdot C_{N,j} \cdot \varpi_{p,j} \tag{D.14}$$

where

- $R_i$  is the response of the aerosol measuring instrument at *i*-voltage of the DEMC;
- $q_a$  is the aerosol air flow rate;
- $W_{p,j}$  is the weighting factor of the measuring instrument for one particle of  $d_j$  with *p* charges;
- $\varpi_{p,j}$  is the weighting factor for the finite width of mobility;

$p = 1, 2, 3, 4$  equivalent to  $j = i + 1, i + 2, i + 3, i + 4$ , respectively. In addition,  $\Phi_{p,j}$  is the ratio of *p* th charged particles to the total particles within the *j* th size range. As a result, Knutson adopted the Boltzmann's distribution law for particle diameters larger than 0,02 μm. The following equations simplified the theory of Gentry *et al.* for the smaller particles:

$$\Phi_p(d) = \left\{ 2 + \left( \frac{0,1}{d} \right) \right\}^{-1,5444} \quad \text{if} \quad p = \pm 1$$

$$\Phi_p(d) = 0 \quad \text{if} \quad |p| > 1 \tag{D.15}$$

Equation (D.14) may be strictly rewritten in the following forms:

$$R(V) = Q_a \sum \int W_p(d) \cdot \Phi_p(d) \cdot C_{N,p}(d) \cdot \Omega(p \cdot Z \cdot A \cdot V) \quad (\text{D.16})$$

$$R(V) = Q_a \sum \sum W_p(d) \cdot \Phi_p(d) \cdot C_{N,p}(d) \cdot \Omega(p \cdot Z \cdot A \cdot V) \quad (\text{D.17})$$

where

$\Omega$  is called the transfer function (see Clause 5);

$A$  within the term for  $\Omega$  is  $L/(\ln r_2/r_1)$ .

Knutson made measurements using 25 voltage steps from 1,902 to 10 000 volts for each flow condition of a DMA and calculated the particle size distribution of  $N(d_j; j = 1 \text{ to } m - 1)$  using Equation (D.13). He actually increased the voltage,  $V_m$ , to a point where the particle concentration became nearly zero, confirming that there were virtually no particles larger than  $d_m$  in his aerosol.

NOTE The procedure in this clause was published by Knutson (1976) [35].

## Annex E (informative)

### Cylindrical DEMC

#### E.1 Geometry of cylindrical DEMC

A schematic diagram of a cylindrical DEMC is shown in Figure E.1. A clean sheath air flow ( $q_1$ ) surrounds the annular region around the centre rod. The aerosol flow ( $q_2$ ) enters as a thin annular flow adjacent to the outer cylinder. While the majority of the flow exits through holes in the bottom closure of the DEMC as excess flow ( $q_4$ ), a fraction ( $q_3$ ) is withdrawn as monodisperse flow through a circumferential slot located near the bottom of the centre electrode. This flow ( $q_3$ ) goes to the aerosol detector. The flow in the DEMC from the point where aerosol enters to the point where  $q_3$  is extracted is laminar. The inner or outer electrode is maintained at a voltage ( $U$ ) while the counter-electrode is grounded. The aerosol sample flow ( $q_2$ ) enters, and the monodisperse flow ( $q_3$ ) leaves through field free regions. Over the effective length ( $L$ ) between the inlet of  $q_2$  and the outlet of  $q_3$ , the particles are exposed to the electric field produced by the voltage ( $U$ ). The dotted lines in Figure E.1 indicate trajectories of charged particles which define the critical mobilities  $Z_1$ ,  $Z_2$ ,  $Z_3$  and  $Z_4$  associated with the instrument, described in Clause E.2.

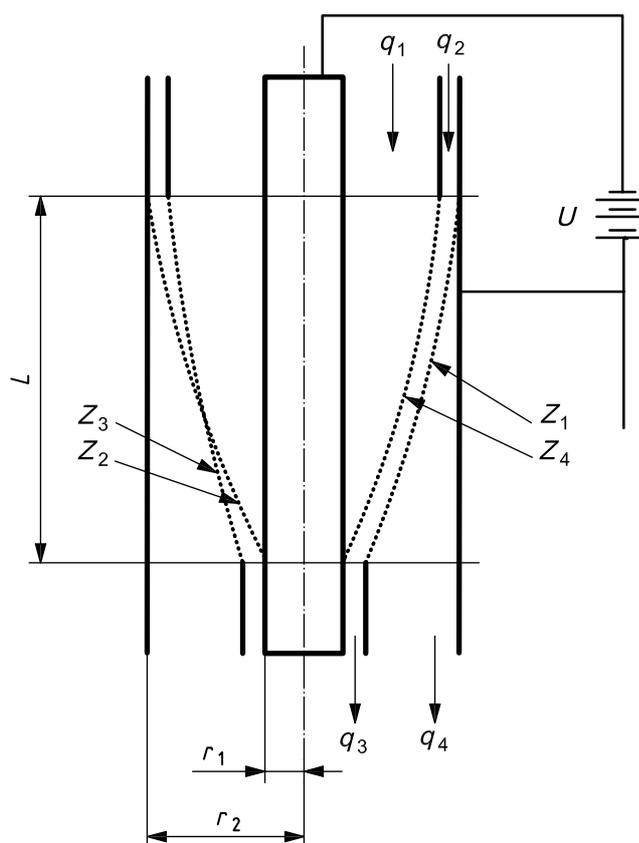


Figure E.1 — Schematic diagram of a cylindrical DEMC

## E.2 Transfer function

The quantities  $Z_1$ ,  $Z_2$ ,  $Z_3$  and  $Z_4$  are the critical mobilities of a charged particle which will follow the critical trajectories shown in Figure E.1. These critical mobilities, determined by the instrument geometry and operating conditions of the DEMC, are given by:

$$Z_1 = \frac{q_1 + q_2 - q_3}{2\pi \cdot \Delta\Phi}, \quad Z_2 = \frac{q_1 + q_2}{2\pi \cdot \Delta\Phi}, \quad Z_3 = \frac{q_1 - q_3}{2\pi \cdot \Delta\Phi}, \quad Z_4 = \frac{q_1}{2\pi \cdot \Delta\Phi} \quad (\text{E.1})$$

where  $\Delta\Phi$  is a function of the geometry and the supply voltage of the DEMC.

For a coaxial cylindrical DEMC,  $\Delta\Phi$  is defined as:

$$\Delta\Phi = \frac{L \cdot U}{\ln\left(\frac{r_2}{r_1}\right)} \quad (\text{E.2})$$

where

$r_1$  and  $r_2$  are the radii of the inner and outer electrodes, respectively;

$L$  is the effective electrode length between the aerosol inlet and outlet;

$U$  is the voltage potential between the electrodes of the DEMC.

If particles of a single mobility,  $Z$ , enter the DEMC, the transfer function  $\Omega(Z)$  is the ratio of the number of particles leaving the DEMC with  $q_3$  to the number of particles with the mobility  $Z$  entering the DEMC with  $q_2$ , or, in other words, the probability that an aerosol particle which enters the DEMC at the aerosol inlet will leave via the detector outlet:

$$\Omega(Z) = \frac{C_{N,3} \cdot q_3}{C_{N,2}(Z) \cdot q_2} \quad (\text{E.3})$$

where  $C_{N,2}$  and  $C_{N,3}$  are the particle number concentrations entering the DEMC with  $q_2$  and leaving the DEMC with  $q_3$ , respectively. If the DEMC is set to the voltage  $U^*$ , the transfer function  $\Omega(Z)$  can be written as:

$$\Omega(Z) = 0 \quad \text{if} \quad Z \leq Z_3 \quad \text{or} \quad Z_2 \leq Z \quad (\text{E.4})$$

$$\Omega(Z) = \frac{1}{q_2} \left[ Z \frac{2\pi \cdot L \cdot U^*}{\ln(r_2/r_1)} - (q_1 - q_3) \right] \quad \text{if} \quad Z_3 \leq Z \leq \min(Z_1, Z_4) \quad (\text{E.5})$$

$$\Omega(Z) = \min\left(1, \frac{q_3}{q_2}\right) \quad \text{if} \quad \min(Z_1, Z_4) \leq Z \leq \max(Z_1, Z_4) \quad (\text{E.6})$$

$$\Omega(Z) = \frac{1}{q_2} \left[ q_1 + q_2 - Z \frac{2\pi \cdot L \cdot U^*}{\ln(r_2/r_1)} \right] \quad \text{if} \quad \max(Z_1, Z_4) \leq Z \leq Z_2 \quad (\text{E.7})$$

The transfer function,  $\Omega(Z)$ , of the DEMC is shown in Figure E.2. The left-hand-side diagram shows the case where  $q_3 > q_2$ ; the centre diagram shows the special case where  $q_3 = q_2$ ; and the right-hand-side diagram shows  $\Omega(Z)$  for  $q_3 < q_2$ .

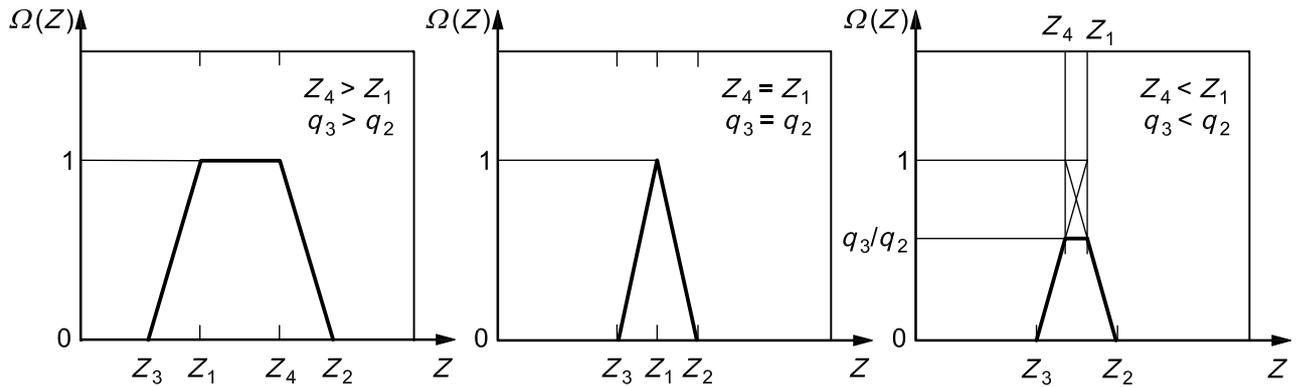


Figure E.2 — Transfer function for a coaxial cylindrical DEMC

The transfer function has the form of a truncated isosceles triangle centred around:

$$Z^* = Z(U^*) = \frac{Z_2 + Z_3}{2} = \frac{Z_1 + Z_4}{2} = \frac{2q_1 + q_2 - q_3}{4\pi \cdot \Delta\Phi} = \frac{q_1 + q_4}{4\pi \cdot L \cdot U^*} \ln(r_2/r_1) \quad (\text{E.8})$$

where

$Z^*$  is the electrical mobility of the target particles;

$U^*$  is the voltage potential on the DEMC that corresponds to the mobility  $Z^*$ .

From Figure E.2 and Equation (E.1), the mobility resolution  $\Delta Z/Z^*$  of the DEMC is defined as:

$$\frac{\Delta Z}{Z^*} = \frac{Z_2 - Z_3}{Z_2 + Z_3} = \frac{q_2 + q_3}{2q_1 + q_2 - q_3} = \frac{q_2 + q_3}{q_1 + q_4} \quad (\text{E.9})$$

In the case of re-circulating the excess flow to the sheath flow ( $q_1 = q_4$ , which forces  $q_2 = q_3$ ), the mobility resolution simplifies to  $\Delta Z/Z^* = q_2/q_1$  with  $Z^* = q_1 \cdot \ln(r_2/r_1) / (2\pi \cdot L \cdot U^*)$ .

If the DMAS is used to measure a particle size distribution, the particles entering the DEMC will not have a single mobility  $Z$ . Instead, a mobility distribution will enter the DEMC. If the mobility distribution function  $f(Z)$  of the aerosol particles entering the DEMC is defined as:

$$f(Z) = \frac{dN_2(Z)}{dZ} \quad (\text{E.10})$$

where  $dN_2(Z)$  is the number concentration of all charged aerosol particles with the opposite polarity of the centre electrode of the DEMC in the mobility range from  $Z$  to  $Z + dZ$ , then the total number concentration of particles  $N_3(U^*)$  leaving the DEMC with the monodisperse flow  $q_3$  is:

$$N_3(U^*) = \frac{q_2}{q_3} \int \Omega(Z, U^*) f(Z) dZ \quad (\text{E.11})$$

With  $\Omega$  from Equations (E.4) to (E.7), Equation (E.11) becomes:

$$N_3(U^*) = \frac{1}{q_3} \left\{ \int_{Z_3}^{Z_a} \left[ Z \frac{2\pi \cdot L \cdot U^*}{\ln(r_2/r_1)} - (q_1 - q_3) \right] f(Z) dZ + \min(q_2, q_3) \int_{Z_a}^{Z_b} f(Z) dZ + \int_{Z_b}^{Z_2} \left[ q_1 + q_2 - Z \frac{2\pi \cdot L \cdot U^*}{\ln(r_2/r_1)} \right] f(Z) dZ \right\} \quad (E.12)$$

where  $Z_a = \min(Z_1, Z_4)$  and  $Z_b = \max(Z_1, Z_4)$ .

Once the air flows are set, any one of the critical mobilities  $Z_1, Z_2, Z_3$  and  $Z_4$  in Equation (E.12) can be taken as an independent variable and is physically varied by changing the voltage,  $U^*$ .

If it is assumed that  $f(Z)$  is nearly constant in the mobility intervals of  $(Z_3, Z_a)$  and  $(Z_b, Z_2)$ , Equation (E.12) reduces to the approximation:

$$N_3(U^*) \cong \min\left(1, \frac{q_2}{q_3}\right) \cdot \left[ \int_{Z_d}^{Z_a} f(Z) dZ + \int_{Z_a}^{Z_b} f(Z) dZ + \int_{Z_b}^{Z_c} f(Z) dZ \right] \cong \min\left(1, \frac{q_2}{q_3}\right) \cdot \int_{Z_d}^{Z_c} f(Z) dZ \quad (E.13)$$

where  $Z_d = \frac{1}{2} \cdot [Z_3 + \min(Z_1, Z_4)]$  and  $Z_c = \frac{1}{2} \cdot [Z_2 + \max(Z_1, Z_4)]$ .

If  $q_1 = q_4$  (which forces  $q_2 = q_3$ ), the mobility  $Z_1$  equals  $Z_4$ . The transfer function becomes symmetrically triangular and Equation (E.13) further reduces to:

$$N_3(U^*) \cong \int_{Z_d}^{Z_c} f(Z) dZ \cong \frac{1}{2} \cdot \int_{Z_3}^{Z_2} f(Z) dZ \quad (E.14)$$

The above analysis is based on the assumptions that

- a) particle inertia and Brownian motion may be neglected,
- b) the air flow is laminar, axi-symmetric and incompressible, and
- c) the space charge and its image forces are negligible.

An analysis including the influence of Brownian motion can, for example, be found in Stolzenburg (1988) [49] or Hagwood *et al.* (1999) [25].

### E.3 Uncertainty calculation for $Z^*$

The influence parameters for the centre particle mobility follow [from Equation (E.8)]:

$$Z^* = \frac{2 \cdot q_1 + q_2 - q_3}{4\pi LU} \cdot \ln\left(\frac{r_2}{r_1}\right) \quad (E.15)$$

This equation describes the static situation of the electrical mobility for the monodisperse aerosol and not the uncertainty in the scanning mode. The following assumptions allow the calculation of the uncertainty of  $Z^*$ . The calculation can be performed with the GUM Workbench Version 2.3.2.36. All uncertainties,  $u_x$ , in  $(x \pm u_x)$  are given as standard uncertainties (coverage factor  $C = 1$ ); the percentage contributions to the total uncertainty are given below.

- Sheath air flow  $q_1 = (3,00 \pm 0,06)$  l/min (volumetric flow, including fluctuation, and deviations due to atmospheric pressure and air temperature) contributes with 88 %.

- Voltage  $U$  (standard uncertainty of 0,5 %, negligible fluctuations) contributes with 6 %.
- Length  $L$  (standard uncertainty of 0,5 %) contributes with less than 1 %.
- Electrode diameters  $r_1$  and  $r_2$  (standard uncertainty of 0,1 % and 0,06 %) contribute with less than 1 %.
- Aerosol air flow  $q_2 = (0,300 \pm 0,006)$  l/min (volumetric flow, including fluctuation, and deviations due to atmospheric pressure and air temperature) contributes with less than 1 %.
- Monodisperse aerosol air flow  $q_3 = (0,300 \pm 0,006)$  l/min (volumetric flow, including fluctuation and deviations due to atmospheric pressure and air temperature, conservative assumption for the correlation between  $q_2$  and  $q_3$  is 0) contributes with less than 1 %.
- The roughness and the soiling of the electrode surface causes an inhomogeneity of the electrical field. This effect is assumed to be included in the uncertainty for  $U$ ,  $r_1$  and  $r_2$ .
- Inhomogeneities of the flow streamlines (due to surface effects) are neglected.

The uncertainty with the above assumptions is  $u_{Z^*} / Z^* = 2,2$  % (slip correction factor  $S_c = 1$ ).

Other uncertainty calculations can, for example, be found in Donnelly and Mulholland (2003)<sup>[16]</sup> and Mulholland *et al.* (2006)<sup>[42]</sup>.

## E.4 Test methods for laminar flow

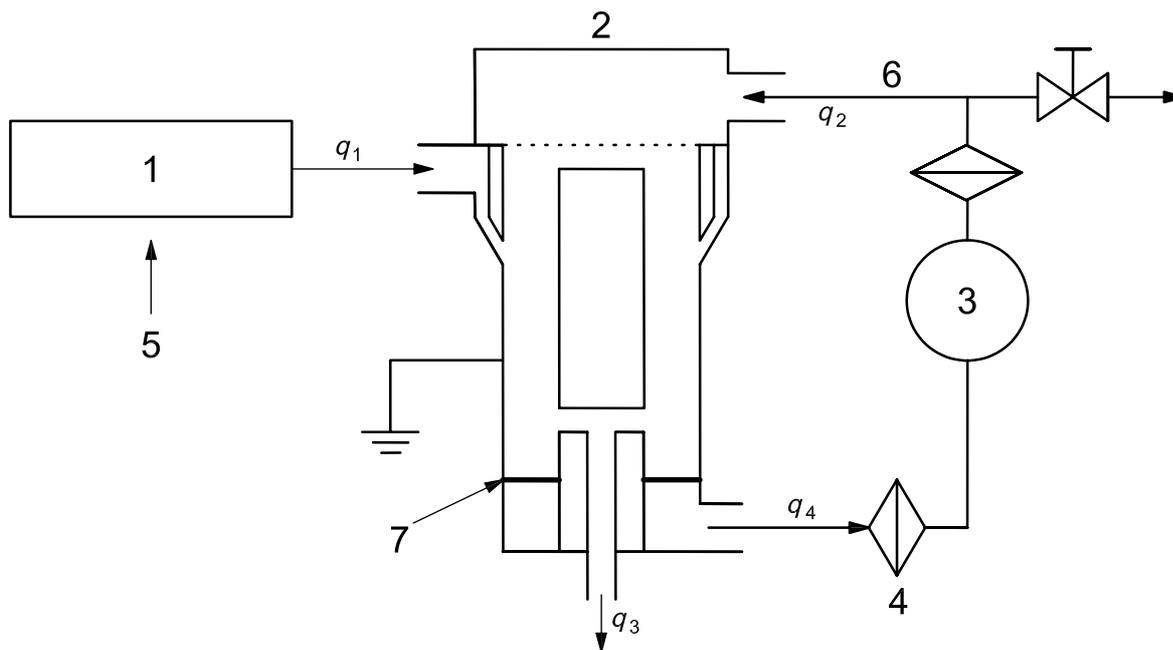
### E.4.1 General

The flow pattern of aerosol and sheath air inside a DEMC strongly influences the performance of the DEMC to obtain the mobility distribution data. If the aerosol and sheath air do not undergo laminar flow, the shape of the mobility distribution and transfer function will be distorted. The DEMC zero test described in 7.3.2 can indicate flow distortions in a DEMC. The method described here can be used by the developer of a DEMC to check for laminar flow.

### E.4.2 Test method

Figure E.3 shows the experimental setup. The setup includes an aerosol generator, clean air feeding device, test DEMC and a filter sheet for flow test. Visualization of the flow distribution in the DEMC annulus is carried out by observing the pattern of collected particles on a filter sheet placed a few millimetres downstream of the aerosol exit slit. A suitable filter sheet is medium performance glass fibre filter with low pressure drop, cut to a suitable size. Solid tracer particles of water soluble, contrasting-colour dyestuff, such as fluorescein, are aerosolized by a nebulizer and introduced into the aerosol inlet of the test DEMC. During normal operation, both the aerosol flow ( $q_2$ ) with tracer particles and the filtered sheath air ( $q_1$ ) are passed through the filter sheet.

Operate the DEMC with normal aerosol and sheath air flow rates and with no voltage across the DEMC for a sufficient time to see the deposit from the particles collected on the filter sheet. Then disassemble the DEMC and observe the pattern of particles collected on the filter sheet to determine whether there was any mixing between the aerosol flow and the sheath air flow.



- Key**
- 1 particle generator
  - 2 test DEMC
  - 3 pump
  - 4 filter
  - 5 clean air
  - 6 sheath air
  - 7 filter sheet for flow test

**Figure E.3 — Experimental setup for checking laminar flow**

The concentricity of the particle deposition pattern and the width of the deposited particle ring help to evaluate if the DEMC is operated with undisturbed laminar flow conditions.

## Annex F (informative)

### Size calibration of a DMAS with step-wise voltage change using particle size standards

#### F.1 General

This annex provides a calibration method that uses size standard particles. The correction considers only errors that arise in the “static” operation of the DMAS, i.e. the operation mode in which the DEMC voltage is changed stepwise during measurements. Correction of errors due to ‘dynamic’ operation of the DMAS, i.e. the operation mode in which the voltage is swept continuously during measurements (so-called “scanning” mode), is not considered here.

It is assumed that flow rates and voltages were calibrated as described in 7.4 and 7.5. This calibration reveals deviations due to either errors in the DEMC dimensions or residual errors in the flow rates (or both). These errors can be corrected by including an appropriate correction factor in the equation that calculates electrical mobility from DEMC parameters. For example, where a cylindrical DEMC is involved, the equation:

$$Z = \zeta \cdot \frac{(2q_1 + q_2 - q_3) \ln(r_2 / r_1)}{4\pi LU} \quad (\text{F.1})$$

can be used (see Annex E), where the correction factor is denoted by  $\zeta$ .

In the calibration method described here, the value of the correction factor is to be determined through measurement of size standard particles by the DMAS under calibration, so that the measured electrical mobility of the standard particles matches the electrical mobility calculated by Equation (1) for the certified size of the standard particles.

The uncertainty associated to the result of the calibration shall be calculated following the procedure described in Clause F.4 and reported. This calculation method is in accordance with the guidelines given in the *Guide to the expression of uncertainty in measurement* [2].

#### F.2 Procedure

Follow the following steps.

- 1) Record the temperature and pressure in the DEMC.
- 2) Aerosolize the particle size standards of which the certified size is traceable to internationally recognized standards.
- 3) Obtain a spectrum of the particle concentration,  $C_N$ , while the voltage,  $U$ , is changed step-wise.
- 4) Calculate the number-weighted mean electrical mobility,  $\bar{Z}$ , from the  $U$ - $C_N$  spectrum obtained in Step 3 by following the procedure in Clause F.3.
- 5) Repeat Steps 3 and 4  $n$  times and obtain the average of the mean electrical mobility,  $\bar{\bar{Z}}$ .
- 6) Calculate the electrical mobility,  $Z_C$ , that corresponds to the certified size,  $d_c$ , of the standard particles by using Equations (1) to (4). Use pressure and temperature obtained in Step 1 in the calculations of the slip correction, viscosity and mean free path.

7) Calculate the correction factor,  $\zeta$ , as:

$$\zeta = \frac{Z_C}{\bar{Z}} \quad (\text{F.2})$$

The standard particles should have a small uncertainty in the particle size and a narrow size distribution. The relative standard uncertainty of the size should be equal to or less than 5 % in diameter, and the relative standard deviation of the distribution should be equal to or less than 20 % in diameter when available.

NOTE It is not required to determine  $\zeta$  at more than one particle size, since the  $\zeta$  value is independent of particle size if the assumption on the sources of sizing errors is correct.

### F.3 Calculation of the number-weighted mean electrical mobility, $\bar{Z}$

Based on the work by Knutson and Whitby (1975) [36], the number-weighted mean electrical mobility,  $\bar{Z}$ , can be calculated from a  $C_N - U$  spectrum as:

$$\bar{Z} = \frac{I_1^*}{N_{in} q_2 \left( \frac{2\pi L}{q_4 \ln(r_2/r_1)} \right) I_1} \quad (\text{F.3})$$

The terms  $q_2$ ,  $q_4$ ,  $L$ ,  $r_1$  and  $r_2$  are defined in 3.2, and the terms  $I_1^*$ ,  $N_{in}$  and  $I_1$  can be calculated using the following equations:

$$I_1^* = \int_0^\infty \frac{N(U)dU}{U^2} \quad (\text{F.4})$$

$$N_{in} = \frac{I_0^*}{q_2 I_0} \quad (\text{F.5})$$

where

$$I_0^* = \int_0^\infty \frac{N(U)dU}{U}$$

and

$$I_0 = [(1 - q_2') \ln(1 - q_2') - (1 + q_3' - q_2') \ln(1 + q_3' - q_2') + (1 + q_3') \ln(1 + q_3')] / q_2'$$

$$I_1 = \frac{1}{q_2'} \ln \frac{1 + q_3' - q_2'}{(1 + q_3')(1 - q_2')}$$

$$q_2' = q_2 / q_4, \quad q_3' = q_3 / q_4$$

( $q_3$ , etc. are defined in 4.1.)

© ISO 2009 – All rights reserved

## F.4 Uncertainty of the result of the calibration

The standard uncertainty of the calibration result using standard-size particles of the certified size,  $d_c$ , denoted by  $u_c(d_c)$ , can be evaluated by taking two uncertainties into consideration:

- 1) the uncertainty of the certified particle size,  $u_{\text{cert}}(d_c)$ , and
- 2) the uncertainty due to random dispersion that occurs in the repeated measurement of  $\bar{Z}$  in determination of the correction factor,  $\zeta$ .

The random dispersion in determination of  $\zeta$  is expressed as the experimental standard deviation of  $\bar{Z}$ ; that is:

$$s(\bar{Z}) = \sqrt{\frac{\sum_{k=1}^n (\bar{Z}_k - \bar{\bar{Z}})^2}{n-1}} \quad (\text{F.6})$$

Convert this experimental standard deviation in electrical mobility,  $s(\bar{Z})$ , to that in particle size,  $s(d_{\bar{Z}})$ , as:

$$s(d_{\bar{Z}}) = s(\bar{Z}) \cdot \left| \frac{d(d)}{dZ} \right|_{d=d_{\bar{Z}}} \quad (\text{F.7})$$

where

$$\begin{aligned} \left| \frac{d(d)}{dZ} \right|_{d=d_{\bar{Z}}} &= \left( \left| \frac{dZ}{d(d)} \right|_{d=d_{\bar{Z}}} \right)^{-1} \\ &= \left( -\frac{Z}{S_c(d_{\bar{Z}}) \cdot d_{\bar{Z}}} \{2S_c(d_{\bar{Z}}) - 1 + BC \exp[-C / Kn(d_{\bar{Z}})]\} \right)^{-1} \\ &\cong \left( -\frac{Z_c}{S_c(d_c) \cdot d_c} \{2S_c(d_c) - 1 + BC \exp[-C / Kn(d_c)]\} \right)^{-1} \end{aligned}$$

(Refer to 4.2 for  $S_c$ ,  $B$ ,  $C$  and  $Kn$ .)

It is assumed in the above calculation that  $d_{\bar{Z}} \cong d_c$  so that the calculation of  $d_{\bar{Z}}$  from  $\bar{Z}$  can be omitted.

Using the experimental standard deviation,  $s(d_{\bar{Z}})$ , the combined standard uncertainty,  $u_c(d_c)$ , is expressed as:

$$u_c(d_c)^2 = u_{\text{cert}}(d_c)^2 + \frac{s(d_{\bar{Z}})^2}{n} \quad (\text{F.8})$$

**NOTE** In the above calculation, the uncertainty of the calibration result is expressed in terms of particle size, rather than in electrical mobility, although a more direct expression of the uncertainty would be that of  $\zeta$ , which is a value defined in the mobility domain. The uncertainty expressed in particle size has the advantage that the uncertainty which arises in conversion between particle size and mobility can be omitted in the calculation of the combined uncertainty, based on the argument by Mulholland *et al.* (2006) [42]. In addition, it is easier for typical users to interpret the value of the uncertainty if it is expressed in terms of particle size.

## Annex G (informative)

### Uncertainty

#### G.1 General considerations

The primary source of uncertainty in a measurement of particle size distribution is often caused by variations of the aerosol concentration and size distribution during the measurement. All such variations will cause errors in the measured size distribution. The discussion below assumes that the aerosol size distribution, including the aerosol concentration, remains constant during the entire scan of the size distribution.

The measurement of the mode of the particle mobility distribution of an aerosol by a DMAS (units  $\text{m}^2 \cdot \text{V}^{-1} \cdot \text{s}^{-1}$ ) is, in principle, traceable to SI via measurements of voltage, dimensions and flow. As long as each instrumental or operational parameter that can affect the transfer function is accurately known, no calibration in terms of particle mobility is needed.

The determination of the curve of a **particle mobility distribution** requires knowledge of the transfer function (see 4.4). The assumptions for the transfer function shall be verified for the particle mobility of interest.

The calculation of the **mobility diameter** from the electrical mobility,  $Z$ , can only be performed with restrictions. The first restriction is that the calculation is only correct for spherical particles. Therefore, the diameter calculated shall be designated as equivalent mobility diameter for spherical particles. The second restriction concerns the uncertainty of the slip correction function  $S_c(d, \lambda, \eta)$  with  $\lambda$  (mean free path length) and  $\eta$  (viscosity of air) as described in Annex C.

The **equivalent mobility diameter**,  $d$ , can be calculated from the measured electrical mobility  $Z$ . For this purpose, the equation  $Z(d, \lambda, \eta)$  must be solved for  $d$ :

$$Z(d, \lambda, \eta) = \frac{p \cdot e \cdot S_c(d, \lambda, \eta)}{3 \cdot \pi \cdot \eta \cdot d} \quad (\text{G.1})$$

where  $p$  is the number of elementary charges,  $e$ , per particle.

The inverse function of  $Z(d, \lambda, \eta)$  shall be named  $d_{cc}(Z, \lambda, \eta)$ .

The scanning mode of the DMAS is a **dynamic measurement**. Additional influence parameters shall be considered, including:

- a) delay time in the DEMC, between the DEMC and particle counter, and in the particle counter;
- b) scanning rate (range of mobility and time); and
- c) contamination of the system by residual particles (during scanning and from one scan to the other).

**Quantitative particle number concentration measurements** can only be measured by a DMAS with restrictions. The efficiency of particle charging (see Annex A), losses of particles in the DEMC, the effective transfer function (see Annex E for a cylindrical DEMC) and knowledge of the slip correction (Annex C) are functions of particle size and instrument construction. Knowledge of these limiting parameters is essential for number concentration measurements.

## G.2 Influence parameters for $Z$

### G.2.1 General

The following paragraphs show the major influence parameters for the measurement of the median particle mobility,  $Z$ . For all parameters, the equation of their influences shall be determined by an equation such as:

$$Z = f(U, q_i, L_i, f_{\text{loss}}, f_{\text{eff.charge}}, f_{\text{eff.det}} \text{ etc}) \quad (\text{G.2})$$

where

$f_{\text{loss}}$  is the fractional loss of particles;

$f_{\text{eff.charge}}$  is the fractional charging efficiency of the particles;

$f_{\text{eff.det}}$  is the fractional detection efficiency of the particles.

The principle and the construction of the DEMC determine this equation. The overall uncertainty,  $u_Z$ , is the result of the uncertainties of each parameter according to the rules of error propagation:

$$u_Z^2 = \left( \frac{\partial f}{\partial U} \cdot u_U \right)^2 + \sum_i \left( \frac{\partial f}{\partial q_i} \cdot u_{q,i} \right)^2 + \sum_i \left( \frac{\partial f}{\partial L_i} \cdot u_{L,i} \right)^2 + \left( \frac{\partial f}{\partial f_{\text{loss}}} \cdot u_{f.\text{loss}} \right)^2 + \sum_i \left( \frac{\partial f}{\partial f_{\text{eff},i}} \cdot u_{f.\text{eff},i} \right)^2 \quad (\text{G.3})$$

Estimations of uncertainties of the following parameters need detailed studies of the DEMC design and experimental examination (see Annex E for a cylindrical DEMC).

### G.2.2 Electrical voltage, $U$ , with uncertainty $u_U$

The electrical voltage,  $U$ , scales directly with the selected particle mobility,  $Z$ . Uncertainties result from the absolute value and the fluctuation of the voltage. Uncertainty of the average voltage propagates directly to uncertainty of the mobility,  $Z$ . Additionally, fluctuation of the voltage causes broadening of the transfer function.

### G.2.3 Flows $q_i$ with uncertainties $u_{q,i}$

The **sheath flow** scales directly with the selected particle mobility,  $Z$ . The sheath flow shall be given as a volume flow. Therefore, ambient pressure and gas temperature are important influence parameters to be considered. The uncertainty of the sheath flow propagates directly to the uncertainty of the particle mobility. Fluctuations of the sheath flow degrade the transfer function and reduce the size resolution.

The **sample flow** is indirectly linked both to particle mobility selection and to particle concentration measurements. The ratio of aerosol flow to sheath flow influences the transfer function width. Higher ratio reduces the size resolution. Fluctuating sample flow degrades the transfer function and reduces the size resolution of the measurement.

Like the sample flow, the **monodisperse aerosol flow** is not directly linked to particle mobility selection, but usually scales directly with particle concentration measurements. Elevated or fluctuating sample flow degrades the transfer function and reduces the size resolution of the measurement. However, the influence is less significant than for elevated or fluctuating sheath flow.

The **aerosol particle detector flow** scales directly with particle concentration measurement. If this flow differs from the monodisperse aerosol flow, the additional supply of air, whether positive or negative, shall be quantified and controlled. Internal bypass or dilution flows within a particle detector shall also be calibrated.

#### G.2.4 DEMC geometry, $L_i$ , with uncertainties $u_{L,i}$

The geometry of a DEMC defines the air flow field, electrical field and particle propagation. This is described with the transfer function (see 4.4). Therefore, the mechanical geometry and its tolerances shall be considered in the uncertainty calculation.

Furthermore, the theoretical transfer function of a DEMC is flattened and broadened due to Brownian diffusion. This effect increases with decreasing particle size. Thus the size resolution of a DEMC is reduced and shall be corrected or considered as an uncertainty.

#### G.2.5 Particle losses $f_{\text{loss}}$ with uncertainty $u_{f,\text{loss}}$

There are several different mechanisms of particle losses to consider: Brownian diffusion of particles to the container walls, particle impaction in sharp bends of the flow, thermophoretic effects, space-charge loss, image-force loss and loss to electrostatically-charged tubes. Particle loss is more important for smaller particles than for larger particles.

Particle losses can either be determined by modelling or by measurement. The size-dependent particle loss correction can be estimated by comparison of the direct measurement of the particle number concentration with a CPC and the integrated total number concentration resulting from the DMAS, using particles of different sizes. The uncertainty,  $u_{f,\text{loss}}$ , results basically from the empirical standard deviation of the measurements.

#### G.2.6 Efficiency factors $f_{\text{eff},i}$ with uncertainty $u_{f,\text{eff},i}$

If the charge distribution achieved by the particle charge conditioner differs from the charge distribution used in the data analysis, this results in erroneous particle distribution and concentration measurement.

The aerosol particle detector efficiency as a function of particle size must be known and included in the data inversion.

It is not possible to cover all possible factors and their determinations in this International Standard, as this requires a detailed knowledge of the equipment being used.

## Bibliography

- [1] ISO 9276-1:1998, *Representation of results of particle size analysis — Part 1: Graphical representation*
- [2] ISO/IEC Guide 98-3, *Uncertainty of measurement — Part 3: Guide to the expression of uncertainty in measurement (GUM:1995)*
- [3] ADACHI, M., DAVID, F.J. and PUI, D.Y.H. (1992). High-efficiency unipolar aerosol charger using a radioactive alpha source. *J. Aerosol Sci.*, **23**, pp. 123-137
- [4] ADACHI, M., KOUZAKA, Y. and OKUYAMA, K. (1985). Unipolar and bipolar diffusion charging of ultrafine aerosol particles. *J. Aerosol Sci.*, **16**, pp. 109-123
- [5] ALLEN, M.D. and RAABE, O.G. (1982). Re-evaluation of Millikan's oil drop data for the motion of small particles in air. *J. Aerosol Sci.* **13**, pp. 537-547
- [6] ALLEN, M.D. and RAABE, O.G. (1985). Slip correction measurements of spherical solid aerosol particles in an improved Millikan apparatus. *Aerosol Sci. Technol.*, **4**, pp. 269-286
- [7] BISKOS, G. (2004). Theoretical and Experimental Investigation of the Differential Mobility Spectrometer. *Dissertation*, University of Cambridge, Cambridge
- [8] BRICARD, J., (1965). *Problems of Atmospheric and Space Electricity*, Elsevier, Amsterdam, pp. 82-117
- [9] BÜSCHER, P., SCHMIDT-OTT, A. and WIEDENSOHLER, A. (1994). Performance of a unipolar "square wave" diffusion charger with variable  $Nt$ -product, *J. Aerosol Sci.*, **25**, pp. 651-664
- [10] CHAPMAN, S. and COWLING, T.G. (1970). *The mathematical theory of non-uniform gases: an account of the kinetic theory of viscosity, thermal conduction and diffusion in gases*. Cambridge University Press, Cambridge
- [11] CHEN, D.-R. and PUI D.Y.H. (1999). A High Efficiency, High Throughput Unipolar Aerosol Charger for Nanoparticles. *J. Nanoparticle Res.*, **1**, pp. 115-126
- [12] COLLINS, D.R., COCKER, D.R., FLAGAN, R.C. and SEINFELD, J.H. (2004). The Scanning DMA Transfer Function. *Aerosol Sci. Technol.*, **38**, pp. 833-850
- [13] CUNNINGHAM, E. (1910). On the Velocity of Steady Fall of Spherical Particles through Fluid Medium. *Proc. Roy. Soc., London*, **A83**, pp. 357-365
- [14] DAVIES, C.N., (1945). Definitive equations for the fluid resistance of spheres. *Proc. Phys. Soc., London*, **57**, Pt. 4, pp. 259-270
- [15] DEMARCUS, W. and THOMAS, J.W. (1952). *Theory of a Diffusion Battery*, ORNL-1413, Oak Ridge National Laboratory, Oak Ridge, Tennessee, p. 26
- [16] DONNELLY, M.K. and MULHOLLAND, G.W. (2003). Particle size measurements for spheres with diameters of 50 nm to 400 nm. *NISTIR 6935*, Building and Fire Research Laboratory; National Institute of Standards and Technology; Gaithersburg, Maryland
- [17] EINSTEIN, A. (1905). Motion of suspended particles from kinetic theory. *Ann. der Phys.*, **17**, pp. 549-560
- [18] FUCHS, N.A. (1947). On the charging of particles in atmospheric aerosols. *Izvestiia Akademii Nauk SSSR. Seriya Geograficheskaya i Geofizicheskaya*, **11**, pp. 341-348 (In Russian)

- [19] FUCHS, N.A. (1963). On the stationary charge distribution on aerosol particles in a bipolar ionic atmosphere. *Geofis. Pura Appl.*, **56**, pp. 185-193
- [20] FUCHS, N.A. (1964). *The Mechanics of Aerosols*, Pergamon Press, Oxford
- [21] FUCHS, N.A. and Sutugin, A.G. (1970). *Highly Dispersed Aerosol*, Ann Arbor Science, Ann Arbor
- [22] GENTRY, J. and BROCK, J.R. (1967). Unipolar Diffusion Charging of Small Aerosol Particles. *J. Chemical Physics*, **47**(1), pp. 64-69
- [23] GUM Workbench (2005). *The "GUM Workbench" program is used to analyse the uncertainty of physical measurements and calibrations. The analysis and computations follow the rules of the "ISO guide to the expression of uncertainty in measurement"*, www.gum.dk
- [24] GUNN, R. (1956). The hyperelectrification of raindrops by atmospheric electric fields. *J. Meteor.*, **13**, pp. 283-288
- [25] HAGWOOD, C., SIVATHANU, Y. and MULHOLLAND, G. (1999). The DMA transfer function with Brownian motion: a trajectory/Monte-Carlo approach. *Aerosol Sci. Technol.*, **30**, pp. 40-61
- [26] HEWITT, G.W. (1957). The charging of small particles for electrostatic precipitation. *Transactions American Institute of Electrical Engineers*, **76**, pp. 300-306
- [27] HOPPEL, W.A. (1978). Determination of the aerosol size distribution from the mobility distribution of the charged fraction of aerosols. *J. Aerosol Sci.*, **9**, pp. 41-54
- [28] HOPPEL, W.A. and FRICK, G.M. (1986). Ion-aerosol attachment coefficients and the steady-state charge distribution on aerosols in a bipolar environment. *Aerosol Sci. Technol.*, **5**, pp. 1-21
- [29] HOPPEL, W.A. and FRICK, G.M. (1990). The nonequilibrium character of the aerosol charge distributions produced by neutralizers. *Aerosol Sci. Technol.*, **12**, pp. 471-496
- [30] HUSSIN, A., SCHEIBEL, H.G., BECKER, K.H. and PORSTENDÖRFER, J. (1983) Bipolar diffusion charging of aerosol particles—I: Experimental results within the diameter range 4–30 nm, *J. Aerosol Sci.*, **14**, pp. 671-677
- [31] HUTCHINS, D.K., HARPER, M.H. and FELDER, R.L. (1995). Slip Correction Measurements for Solid Spherical Particles by Modulated Dynamic Light Scattering. *Aerosol Sci. Tech.* **22**, pp. 202-218
- [32] KENNARD, E.H. (1938). *Kinetic Theory of Gases*, McGraw-Hill, New York, p. 483
- [33] KIM, J.H., MULHOLLAND, G.W., KUKUCK S.R. and PUI, D.Y.H. (2005). Slip Correction Measurements of Certified PSL Nanoparticles Using a Nanometer Differential Mobility Analyzer (Nano-DMA) for Knudsen Number From 0.5 to 83. *J. Res. Natl. Inst. Stand. Technol.* **110**, pp. 31-54
- [34] KNUDSEN, M. and WEBER, S. (1911). Luftwiderstand gegen die langsame Bewegung kleiner Kugeln. *Ann. d. Phys.* **36**, pp. 981-994
- [35] KNUTSON, E.O. (1976). Extended electrical mobility method for measuring aerosol particle size and concentration. *Fine Particles*, edited by B.Y.H. Liu, pp. 739-762, Academic Press, New York.
- [36] KNUTSON, E.O. and WHITBY, K.T. (1975). Accurate Measurement of Aerosol Electric Mobility Moments. *J. Aerosol Sci.*, **6**, pp. 453-460
- [37] LIU, B.Y.H., WHITBY, K.T. and YU, H.H.S. (1967). Electrostatic aerosol sampler for light and electron microscopy. *Rev. of Sci. Instruments*, **38**, pp. 100-102
- [38] MARLOW, W.H. and BROCK, J.R. (1975). Unipolar charging of small aerosol particles. *J. Colloid and Interface Sci.*, **50**(1), pp. 32-38

- [39] MEDVED, A., DORMAN, F., KAUFMAN, S.L. and PÖCHER A. (2000). A new corona-based charger for aerosol particles, *J. Aerosol Sci.*, **31**, pp. S616-S617
- [40] MILLIKAN, R.A. (1910). The isolation of an ion, a precision measurement of its charge, and the correction of Stoke's law. *Science* **32**, pp. 436-448
- [41] MILLIKAN, R.A. (1923). The general law of fall of a small spherical body through a gas and its bearing upon the nature of molecular reflection from surfaces. *Phys. Rev.* **22**, pp. 1-23
- [42] MULHOLLAND, G.W., DONNELLY, M.K., HAGWOOD, C., KUKUCK, S.R., HACKLEY, V.A. and PUI, D.Y.H., (2006). Measurement of 100 nm and 60 nm particle standards by differential mobility analysis. *J. Res. Natl. Inst. Stand. Technol.*, **111**, pp. 257-312
- [43] PORSTENDÖRFER, J., HUSSIN, G., SCHEIBEL, H.G. and BECKER, K.H. (1983). Bipolar diffusion charging of aerosol particles. *J. Aerosol Sci.*, **14**, pp. 127-133
- [44] PUI, D.Y.H. (1976). *Experimental Study of Diffusion Charging of Aerosols*. Ph.D. thesis, Mechanical Engineering Department, University of Minnesota, Minneapolis
- [45] PUI, D.Y.H., Fruin, S. and McMurry, P.H. (1988). Unipolar diffusion charging of ultrafine aerosols. *Aerosol Sci. Technol.*, **8**(2), pp. 173-187
- [46] RADER, D.J. (1990). Momentum slip correction factor for small particles in nine common gases. *J. Aerosol Sci.*, **21**, pp. 161-168
- [47] REIF, A.E. (1958). In: *Aviation Medicine Selected Reviews*, C.S. White, W.R. Lovelace II and F.G. Hirsch, eds., Pergamon Press, Oxford, pp. 168-244
- [48] REISCHL, G.P., MÄKELÄ, J.M., KARCH, R. and NECID, J. (1996). Bipolar charging of ultrafine particles in the size range below 10 nm. *J. Aerosol Sci.*, **27**(6), pp. 931-949
- [49] STOLZENBURG, M.R. (1988). *An ultrafine aerosol size distribution measuring system*. Ph.D. thesis, University of Minnesota, Minneapolis, MN
- [50] WIEDENSOHLER, A. (1988). An approximation of the bipolar charge distribution for particles in the submicron range. *J. Aerosol Sci.*, **19**(3), pp. 387-389
- [51] WIEDENSOHLER, A. and FISSAN, H.J. (1991). Bipolar charge distribution of aerosol particles in high purity argon and nitrogen. *Aerosol Sci. Technol.*, **14**, pp. 358-364
- [52] WIEDENSOHLER, A., LÜTKEMEIER, E., FELDPAUSCH, M. and HELSPER, C. (1986). Investigation of the bipolar charge distribution at various gas conditions. *J. Aerosol Sci.*, **17**, pp. 413-416
- [53] DAHNEKE, B. (1973). Slip correction factors for nonspherical bodies — Introduction and continuum flow. *J. Aerosol Sci.*, **4**, pp. 139-145
- [54] MATTAUCH, J. (1925). An experimental announcement on the resistance principle of small spheres in gases. *Zeitschrift für Physik*, **32**, May-June 1925, pp. 439-472
- [55] SCHMIDT, K.H. (1959). Untersuchungen an Schwebstoffteilchen im Temperaturfeld. *Z. Naturforsch.*, **14a**, pp. 870-881

